Seasonal, Diurnal, and Tidal Variations of Dissolved Inorganic Carbon and pCO2 in Surface Waters of a Temperate Coastal Lagoon (Arcachon, SW France)

Pierre Polsenaere, Bruno Delille, Dominique Poirier, Céline Charbonnier, Jonathan Deborde, Aurélia Mouret, Gwenaël Abril

Seasonal, diurnal and tidal variations of dissolved inorganic carbon and pCO_2 in surface waters of a temperate coastal lagoon (Arcachon, SW France)

Pierre Polsenaere[1,2*], Bruno Delille[3], Dominique Poirier[1], Céline Charbonnier[1], Jonathan Deborde[1,2], Aurélia Mouret[1,4] and Gwenaël Abril[1,5,6]

[*]Corresponding author: Pierre.Polsenaere@Ifremer.fr

[1] Laboratoire Environnements et Paléoenvironnements Océaniques et Continentaux (EPOC), CNRS-UMR 5805, Université de Bordeaux, France.

[2] IFREMER, Littoral, Laboratoire Environnement et Ressources des Pertuis Charentais (LER-PC), BP133, 17390, La Tremblade, France.

[3] Unité Océanographie Chimique, Département d'Astrophysique, Géophysique et Océanographie, Université de Liège, Allée du 6 Août, 17-Bât. B5 4000 Liège, Belgium.

[4] UMR 6112 LPG-BIAF Recent and Fossil Bio-Indicators, Angers University, 2 Bd Lavoisier, F-49045, Angers, France.

[5] Laboratoire de Biologie des Organismes et Écosystèmes Aquatiques (BOREA), UMR CNRS 8067, Muséum National d'Histoire Naturelle, 61 rue Buffon, 75231, Paris cedex 05, France.

[6] Programa de Biologia Marinha e Ambientes Costeiros, Universidade Federal Fluminense, Outeiro São João Batista s/n, 24020015, Niterói, RJ, Brazil.

A research paper published in Estuaries and Coasts

Key words: coastal zone; dissolved inorganic carbon; water pCO_2; water-air CO_2 fluxes; tidal, diurnal, seasonal variations; physical, biological, chemical processes.

Abstract

We report on diurnal, tidal and seasonal variations of dissolved inorganic carbon (DIC), water partial pressure of CO_2 (pCO_2) and associated water-air CO_2 fluxes in a tidal creek of a temperate coastal lagoon with 70 % of intertidal flats, during eight tidal/diurnal cycles and two consecutive years covering all seasons. Surface waters of the lagoon were always slightly oversaturated in CO_2 with respect to the atmosphere with an average pCO_2 value of 496 ± 36 ppmv. Seasonally, subsurface water pCO_2 values were controlled by both temperature and biological / tidal advection effects that compensated each other and resulted in weak annual variations. High-resolution temporal pCO_2 records reveal that highest fluctuations (192 ppmv) occurred at the tidal/diurnal scale as a result of biological activity, advection from the tidal flat and porewater pumping that all contributed to water pCO_2 and carbonate chemistry variations. Total Alkalinity (TA) versus salinity plots suggest a net production of alkalinity in the lagoon attributed to benthic carbonate dissolution and/or anaerobic degradation of organic matter. We specifically highlighted that for a same salinity range, during flooding, daytime pCO_2 were generally lower than nighttime pCO_2 values because of photosynthesis, whereas during ebbing, daytime pCO_2 were higher than nighttime pCO_2 values because of heating. Waters in the lagoon were a relatively weak CO_2 source to the atmosphere over the year compared to other estuarine and lagoon waters elsewhere, and to sediment-air fluxes measured simultaneously by atmospheric Eddy Covariance (EC) in the Arcachon lagoon. Because of low values and small variations of the air-sea pCO_2 gradient, the variability of fluxes calculated using the piston velocity parameterization was greatly controlled by the wind speed at the diurnal and, to a lesser extent, seasonal time scales. During the emersion, the comparison of these pCO_2 data in the tidal creek with EC fluxes measured 1.8 km away on the tidal flat suggests high heterogeneity in air-sea CO_2 fluxes, both spatially and at short time scales according to the inundation cycle

and the wind speed. In addition to tidal pumping when the flat becomes emerged, our data suggest that lateral water movement during the emersion of the flat generates strong spatial heterogeneity in water-air CO_2 flux.

1. Introduction

Coastal zones represent key systems in biogeochemical cycle couplings between land, oceans and the atmosphere, processing considerable amounts of matter, energy and nutrients (Borges et al. 2005; Cole et al. 2007; Cai 2011). Despite its relatively modest surface area (7 % of the global ocean surface), the coastal zone accounts for 14-30 % of all oceanic primary production and 90 % of sedimentary organic carbon mineralization (Gattuso et al. 1998; Mantoura et al. 1991; Pernetta and Milliman 1995). Carbon fluxes within and between coastal subsystems and their alteration by climate and anthropogenic changes are substantial. It is essential to understand and accurately account for the factors regulating these fluxes and how they affect the ocean and global carbon budgets (Bauer et al. 2013).

The coastal ocean consists of different but tightly connected ecosystems including estuaries, tidal wetlands, lagoons and the continental shelf. Global CO_2 emissions from estuaries have been estimated at 0.2-0.4 Pg yr^{-1} (Cai 2011; Borges and Abril 2011; Borges et al. 2005; Laruelle et al. 2010), with fluxes disproportionally high in comparison with their global ocean area portion (near 0.2 %). To the contrary, other coastal systems such as tidal wetlands and continental shelves fix 0.55 and 0.25 Pg yr^{-1} of atmospheric CO_2 respectively (Bauer et al. 2013). The spatiotemporal heterogeneity and complexity of coastal systems in terms of carbon processes and fluxes make difficult to precisely quantify each sub-system's carbon balance. For instance, carbon fluxes in tidal systems such as estuaries and small deltas are relatively well characterized (Laruelle et al. 2010; Borges and Abril 2011; Chen et al. 2013). To the contrary, other systems such as fjords, lagoons and marine embayments are neglected despite a large

relative surface among coastal systems, a generally high net primary production and a strong sensitivity to eutrophication phenomenon (Kjerfve 1985; Caumette et al. 1996; Koné et al. 2009; Polsenaere et al. 2012a; Cotovicz et al. 2015). As a consequence, carbon flux measurements are needed for an accurate estimate of global and regional carbon budgets.

In coastal ecosystems, dissolved inorganic carbon (DIC) concentrations, and particularly partial pressures of CO_2 (pCO_2) are driven by several thermodynamic and biotic factors, induced by river water inputs, tidal exchanges, mixing of water masses, photosynthesis and aerobic/anaerobic degradation of organic matter, precipitation/dissolution of calcium carbonate, benthic/pelagic couplings and air-water exchanges (Cai 2011; Gazeau et al. 2004; Cotovicz et al. 2015; Ribas-Ribas et al. 2011). Efforts have been made to understand the seasonal and inter-annual processes affecting carbon system dynamics over coastal ecosystems (Yates et al. 2007). Seasonal measurements of the carbonate system parameters (pCO_2, Total Alkalinity, DIC, and/ or pH) have been performed for instance across salinity gradient transects or strategically located stations along lagoon channels or estuaries (Frankignoulle et al. 1996; Cai et al. 1999; Koné et al. 2009; Ribas-Ribas et al. 2011; Burgos et al. 2018; Wang et al. 2018; Vaz et al. 2019). The influence of smaller-scale rhythms (tidal and diurnal variations) on seasonal and annual carbon dynamics and budgets has also been studied through direct diurnal cycles for instance over east monsoon coastal systems and subtropical bays (Dai et al. 2009; Yates et al. 2007), temperate sea, lagoon, estuary, river, channel and creek (Saderne et al. 2013; Bozec et al. 2011; Borges and Frankignoulle 1999; Ribas-Ribas et al. 2013; Burgos et al. 2018), sub-Antarctic island coastal waters (Delille et al. 2009), tropical and equatorial mangrove waters (Maher et al. 2013; Bouillon et al. 2007; Borges et al. 2003) and continental and subtropical saltmarsh and marsh-dominated estuary systems (Wang and Cai, 2004; Wang et al. 2016; Wang et al. 2018). For instance, in a tidal creek among the Duplin River salt marsh-estuary coastal ecosystem (Georgia, USA), Wang et al. (2018) measured strong seasonal and

tidal/diurnal pCO_2 variations with values ranging from 500 ppmv at high tide to 4000 ppmv at low tide and to 1600 ppmv at high tide to 12,000 ppmv at low tide during coldest and warmest months, respectively. Horizontal advection with river water entrance to the creek at high tide was mentioned to explain lower measured values. To the contrary, for higher values observed at low tide, creek bank pore-water drainage associated to tidal pumping process, as observed over mangroves or wetlands (Maher et al. 2013; Neubauer and Anderson 2003) was highlighted (Wang et al. 2018). Over tidally-influenced shallow systems, all these processes are generally but differently involved and can in turn significantly and specifically influence atmospheric CO_2 fluxes.

CO_2 fluxes at the water-air interface can be measured directly using the Eddy Covariance (Zemmelink et al. 2009; Polsenaere et al. 2012a), floating chambers (Frankignoulle et al. 1998) or be calculated from water pCO_2 measurements and a given gas transfer velocity. CO_2 flux computations can be subject to large uncertainties because of the difficulty in accurately assessing the gas transfer velocity (Raymond and Cole 2001, Vachon et al. 2010). This bias is potentially more important when the water-air CO_2 gradient is small. Diurnal and tidal variations in water pCO_2 of dynamic coastal ecosystems can even add uncertainties on air-sea CO_2 flux estimations. For example, in the Guadalquivir estuary, Ribas-Ribas et al. (2013) observed pCO_2 values fluctuating from source to sink over the same tidal cycle.

In the present study we report tidal, diurnal and seasonal dynamics of inorganic carbon and associated air-sea CO_2 fluxes in a tidal creek of the temperate coastal Arcachon lagoon (SW France). The lagoon is a typical tidal flat of the French Atlantic coast subjected to both marine and continental influences. A complex channel and tidal creek waters network drains the tidal flat during ebb tides. Tidal pumping through anoxic pore-water seeping from mud sediments to tidal creek waters is an important component of the biogeochemical functioning of the lagoon in terms of nutrient dynamics (Deborde et al., 2008a). In this paper, DIC parameters and

100 associated water-air CO_2 fluxes as estimated based on several *in situ* tidal/diurnal cycles (six
101 24-hour and two 12-hour cycles) carried at different seasons during two years (2008 and 2009)
102 are presented. We describe and explain small-scale (diurnal and tidal) and seasonal pCO_2
103 variability along with relevant environmental controls in studied tidal creek waters. We
104 compute air-sea CO_2 fluxes, and discuss associated variability according to small (diurnal and
105 tidal) and seasonal scales and also methodology from coastal regional/global carbon budgets
106 point of view. The computed water-air CO_2 fluxes estimated during these tidal/diurnal cycles
107 are also compared with those measured in summer 2008 by atmospheric Eddy Covariance (EC)
108 over the tidal flat (Polsenaere et al. 2012a).
109
110 **2. Materials and Methods**
111 **2.1. Study area**
112 The Arcachon bay is a temperate macro-tidal lagoon of 174 km^2 on the southwestern Atlantic
113 coast of France (44°40' N, 01°10' W) (Fig. 1). Several studies have focused on the system in
114 particular its hydrodynamics through modelling simulations (Plus et al. 2009; Fauvelle et al.
115 2018); Zostera seagrass meadow dynamic (Auby and Labourg 1996; Plus et al. 2010; Cognat
116 et al. 2018) and relationships with sediment hydrodynamics or redox status (Ganthy et al. 2013;
117 Delgard et al. 2013; Deborde et al. 2008a,b); nutrient and carbon dynamics and export from the
118 Arcachon catchment through *in situ* adapted sampling and modelling strategies (Auby et al.
119 1994; Rimmelin et al. 1998; Canton et al. 2012; Polsenaere et al. 2012b; Polsenaere and Abril
120 2012); and in terms of benthic and pelagic primary production measurements through various
121 *in situ*, laboratory and modelling approaches (Polsenaere et al. 2012a; Migné et al. 2016; Glé
122 et al. 2008; Plus et al. 2015).
123 This triangle-shaped bay is surrounded by the coastal plain of the *Landes de Gascogne*, and
124 communicates with the Atlantic Ocean through a narrow channel 8 km in length (Fig. 1). With

125 a mean depth of 4.6 m, the shallow lagoon presents semi-diurnal tides with amplitudes varying
126 from 0.8 to 4.6 m (Plus et al. 2009). During a tidal cycle, the flat exchanges approximately 264
127 $\times 10^6$ m^3 and 492 $\times 10^6$ m^3 of water with the ocean, respectively during average neap and spring
128 tides. The flushing time of the lagoon ranges between 12.4 and 17.4 days in winter and summer
129 respectively (Plus et al. 2009). Water temperatures in the lagoon vary from 6 °C in winter to
130 22.5 °C in summer, and water salinity varies from 22 to 35 according to freshwater input
131 variations during the year.
132 The flats are tidally submerged by relatively saline waters, and receive moderate amounts of
133 freshwater with an annual input of 813 $\times 10^6$ m^3 (1.8 $\times 10^6$ m^3 at each tidal cycle), of which 8
134 % is from groundwater, 13 % is from rainfall and 79 % is from rivers and small streams
135 (Rimmelin et al. 1998). In total, the carbon export from the watershed to the Arcachon lagoon
136 was estimated at 15,870 t C yr^{-1} or 6 t C km^{-2} yr^{-1}, mostly in the form of dissolved organic
137 carbon (DOC) (35 %), DIC (24 %) as excess CO_2 and $DIC_{equilibrium}$ (i.e. the theoretical DIC
138 concentration at the atmospheric equilibrium), and dissolved CO_2 rapidly lost as degassing to
139 the atmosphere (34 %) (Polsenaere et al. 2012b). Tidal pore-water drainage at low tide is not
140 documented for carbon, but contributes to respectively 55 and 15 % of the dissolved inorganic
141 phosphate (DIP) and nitrate (DIN) input to the lagoon waters (Deborde et al. 2008a).
142 The lagoon surface is composed of 57 km^2 of channels (33 % of the lagoon surface area), with
143 a maximum depth of 25 m at the mouth of the lagoon. These channels drain a large muddy tidal
144 flat of 117 km^2 (67 % of the lagoon). *Zostera noltei* seagrass beds are particularly extensive and
145 colonize up to 60 % of this intertidal area (i.e. 70 km^2) between −1.9 m and +0.8 m relative to
146 local Mean Sea Level (Amanieu, 1967). Annual mean net primary production of *Zostera noltei*
147 expressed as carbon fixation was estimated at 362.9 ± 88.1 t C km^{-2} yr^{-1} (Ribaudo et al. 2017).
148 Polsenaere et al. (2012a) and Migné et al. (2016) gave annual values of the same order of
149 magnitude through atmospheric EC and benthic chamber measurements with 456 and 263 t C

150 km^{-2} yr^{-1} respectively. However, seagrass beds in the lagoon declined by 33 % since the end of
151 the 80's whereas the exact causes remain unclear, leading to a C fixation decline from 24846 ±
152 6030 t C yr^{-1} (1989) to 16564 ± 4020 t C yr^{-1} (2007) (Plus et al. 2009; Plus et al. 2015; Ribaudo
153 et al. 2017). The microphytobenthic (MPB) communities also represent a significant proportion
154 of the total benthic primary production, which is estimated at between 104-114, 628 and 788 t
155 C km^{-2} yr^{-1} (Auby personal communication; Polsenaere et al. 2012a; Migné et al. 2016).
156 Together, these two categories of benthic primary production represent more than half of the
157 total primary production of the flat. Annual integrated phytoplankton primary production has
158 been estimated at 103 t C km^{-2} yr^{-1} which could represent 30 % of the total primary production
159 of the lagoon and places Arcachon within the low to moderate phytoplankton primary
160 production systems (Glé et al. 2008). Microphythobenthic resuspension is also supposed to
161 significantly contribute to planktonic production in Arcachon as highlighted by Savelli et al.
162 (2019) on the Brouage mudflat of the Marennes-Oléron Bay up North along the French Atlantic
163 coast with a 43 % resuspended MPB primary production at this location. The presence of
164 circular tidal pools on the flat also contributes to the biogeochemical functioning of Arcachon
165 bay especially at tidal and diurnal scales (Rigaud et al. 2018) through large spatio-temporal
166 variations in water temperature and irradiance influencing MPB activity and benthic oxygen,
167 nutrients, and reduced compound fluxes.
168 Finally, net CO_2 fluxes between the lagoon and the atmosphere measured at the ecosystem scale
169 by atmospheric EC generally showed small negative (influx) and positive (efflux) values (-13
170 µmol m^{-2} s^{-1} for influxes and 19 µmol m^{-2} s^{-1} for effluxes). Emersion during the day was almost
171 always associated with a net uptake of atmospheric CO_2 due to an enhanced benthic primary
172 production at low tide. In contrast, during immersion (day and night) and emersion at night,
173 CO_2 fluxes were positive, negative or close to zero, depending on the season and the study site
174 (Polsenaere et al. 2012a).

175 **2.2. Sampling strategy and laboratory analysis**

176 In total, six 24-hour cycles (April, July, September 2008, and April, June and September 2009)
177 and two 12-hour cycles (November 2008 and January 2009) were carried out in a subtidal creek
178 at the centre of the lagoon (Fig. 1). For each cycle, water height (H), salinity (S), temperature
179 (T), partial pressure of CO_2 in the water (pCO_2), total alkalinity (TA) and dissolved inorganic
180 carbon isotopic ratio (δ^{13}C-DIC) were measured at the subsurface (0.5 m depth). T and S were
181 measured every minute with an YSI multiparameter probe on board and H was measured every
182 hour by the SHOM (Service Hydrographique et Océanographique de la Marine) at Arcachon
183 (Eyrac pier, 44°39.9001'N 01°09.8130'W). Before each cycle, the salinity (conductivity)
184 sensor was checked and calibrated with 10 and 50 mS cm^{-1} solutions. Water pCO_2 was
185 measured every minute with a marble-type equilibrator system (Frankignoulle et al. 2001;
186 Polsenaere et al. 2012b). An Infra-Red Gas Analyzer (LI-COR, LI-820) was used to measure
187 the pCO_2 in dry air equilibrated with seawater. The LI-820 was calibrated at the laboratory one
188 day before the field experiment using three gas standards of 0, 500 ± 10 ppm and 2959 ± 59
189 ppm. The equilibrator consists of a Plexiglas cylinder (height: 90 cm, diameter: 16 cm) that is
190 filled with marbles to increase the exchange surface area. Water pumped by a peristaltic pump
191 (Masterflex, 1 L min^{-1}), runs from the top to the bottom of the equilibrator, and air is pumped
192 upwards (1 L min^{-1}). The pCO_2 of air equilibrates with the pCO_2 of water and is then measured
193 by the LI-COR after being dried by a Dierite grain tube. Response time of the equilibrator as
194 determined in the laboratory is shorted than 5 minutes (Cotovicz et al. 2016).

195 Discrete water samples were also taken every hour of the tidal cycle for TA and δ^{13}C-DIC in
196 the channel subsurface waters by using a 5L Niskin sampler. Total alkalinity (TA) was
197 measured by titration with HCl 0.1 N on 100 mL filtered samples and was calculated by a Gran
198 function linearisation (Gran 1952) between pH 4.2 and 3. The reproducibility between the
199 measures was better than ±5 μmol kg^{-1}. Accuracy of TA measurements was checked on regular

titrations of a secondary standard of 0.2 µm filtered seawater with a well-known TA concentration, previously calibrated by comparison with a standard from Scripps Institution of Oceanography. The δ^{13}C-DIC measurements were made following Gillikin and Bouillon (2007). In 100 mL vials that were filled to the top, a headspace was first created with Helium gas to obtain a volume of approximately 20 % of the total volume of the vial. Then, 0.3 mL of warm 85 % phosphoric acid was added to transform the carbonate forms into CO_2. To ensure gas equilibration, the vials were shaken and placed upside down for 1.5 h. Measurements were performed by coupling an elemental analyzer (EA; Carlo Erba NC2500) to an Isotope Ratio Mass Spectrometer (IRMS; Micromass Isoprime) equipped with a manual gas injection. We injected 3 mL of headspace gas from the vial headspace. δ^{13}C-DIC was calibrated against a laboratory standard (45 mg of Na_2CO_3 were dissolved in a sealed vial flushed with He gas, with 3 mL of warm 85 % phosphoric acid H_3PO_4). This standard had been calibrated against a certified standard (NBS19, -1.96 ‰) using a dual-inlet IRMS. The isotopic value of the standard Na_2CO_3 was -4.5 ± 0.2 ‰. Finally, the equation of Miyajima et al. (1995) was applied to correct for the isotopic fractionation of the CO_2 between the headspace and the water phase and to calculate the δ^{13}C of the total DIC. The repeatability was approximately ±0.1 ‰ between samples. The stable isotopic composition of DIC (δ^{13}C-DIC) varies over a large range in terrestrial and coastal waters since carbon reservoirs that act as a source of DIC (soil, groundwater, bedrocks and atmosphere) have distinct isotopic signatures (Yang et al. 1996). The δ^{13}C of atmospheric CO_2 is about -7.5 ‰, whereas carbonate rocks have a δ^{13}C of about 0 ‰ (Mook et al. 1983). In a system where soil CO_2 is primarily derived from decomposition of plant organic matter, the CO_2 produced has a $\delta^{13}C–CO_2$ value close to the initial substrate (i.e., -30 to -24 ‰ int the case of C3 plants and -16 to -10 ‰ in the case of C4 plants). Aquatic primary production, in contrast, tends to increase δ^{13}C-DIC and generate strong diel variations

224 (Parker et al. 2005). Finally, gas exchange along subsurface waters generates an isotopic
225 equilibration with the atmosphere and makes the δ^{13}C-DIC less negative.
226
227 **2.3. Calculations and statistical analysis**
228 Dissolved inorganic carbon (DIC) concentrations and species (bicarbonate HCO_3^- and
229 carbonate CO_3^{2-} ions) were calculated from the measured salinity, temperature, pCO_2 and TA
230 using the carbonic acid constants sets from by Mehrbach et al. (1973) as modified by Dickson
231 and Millero (1987), the borate acidity constant from Lee et al. (2010), the K_{HSO4} constant from
232 Dickson (1990) and the CO_2 solubility coefficient of Weiss (1974). The CO_2 System
233 Calculation program (version 2.1.) developed by Lewis and Wallace (1998) performed all
234 calculations.
235 Seasonal temperature ($TpCO_2$) versus non-temperature ($NpCO_2$) effects on measured water
236 pCO_2 during the eight tidal cycles were studied applying equations from Takahashi et al. (2002)
237 as follows:
238 $$TpCO_2 = pCO_{2mean} \times \exp[0.0423(T_{obs} - T_{mean})] \quad (1)$$
239 $$NpCO_2 = pCO_{2obs} \times \exp[0.0423(T_{mean} - T_{obs})] \quad (2)$$
240 Where pCO_{2obs}, T_{obs}, pCO_{2mean}, T_{mean} are respectively the measured pCO_2, temperatures at each
241 time step and the annual mean pCO_2 and temperature calculated across the whole measured
242 dataset. $TpCO_2$ indicates the pCO_2 variations around the mean pCO_2 that would be expected
243 only from temperature fluctuations that occurred over the sampling period (2008-2009). $NpCO_2$
244 represent pCO_2 variations due to biological activity or non-temperature effects (advection, tidal
245 pumping and benthic-pelagic coupling). The constant 0.0423 corresponds to the temperature
246 effect on pCO_2 in isochemical conditions (qln pCO_2/qT), i.e. +4.23 % °C^{-1}.
247 Gas transfer velocities (k_{600}) and air-sea CO_2 fluxes for the eight tidal cycles were computed
248 each hour at high-tide day and night periods. Wind speed values normalized to a 10 meters

height (U_{10}) values were computed from wind speed values measured at 9 meters high by the Lège-Cap Ferret Meteo-France station (44°37.900'N 01°14.900W, 12.5 km far from the 24-H site, Fig. 1) using the Amorocho and DeVries (1980) equation. Gas transfer velocities (k) were estimated according to parameterizations of Wanninkhof et al. (1992), Raymond and Cole (2001) and Abril et al. (2009), noted W92, RC01 and A09, respectively. The W92 equation has been proposed for oceanic water, whereas the RC01 and A09 equations were developed for estuarine waters. For the latter equation, hourly suspended particulate matter (SPM) concentrations measured during every cycle (data not shown) and bottom water velocity currents estimated with the hydrodynamic model from Ifremer (MARS3D, Lazure and Dumas, 2008) were used. Air-sea CO_2 fluxes were then calculated from k, water and air pCO_2 values. The gas transfer coefficients normalized to a Schmidt number of 600 (k_{600}) estimated with the three parameterizations were converted to the gas transfer velocity of CO_2 (k) at *in situ* temperature and salinity following the procedure of Jähne et al. (1987). Air-water CO_2 fluxes were estimated using the formulation as followed:

$$F_{CO2}=\boldsymbol{\alpha} k \Delta pCO_2 \quad (3)$$

where F_{CO2} is the vertical CO_2 exchange at the air-water interface, $\boldsymbol{\alpha}$ is the CO_2 solubility coefficient (Weiss 1974), k is the gas transfer velocity, and ΔpCO_2 is the gradient between water pCO_2 measured by the equilibrator and air pCO_2 set to a mean value of 390 ppm according to simultaneous Eddy Covariance (EC) measurements done in the lagoon (44°42.9858'N 01°08.6160'W, 1.829 km far from the 24-H site, Fig. 1) in 2008 and 2009 (Polsenaere et al. 2012a). For comparison, U_{10} and air-sea CO_2 flux values obtained in July 2008 from simultaneous EC measurements (Polsenaere et al. 2012a) and water carbon parameters (pCO_2) during the July 2008 cycle are also presented.

Data post-processing (graphs and statistics) was performed using the GraphPad Prism version 6.00 software (La Jolla California USA, www.graphpad.com). The Shapiro-Wilk test was used

to test the normality of the data (p-value below 0.05). Due to non-normality of our data, Mann-Whitney and Kruskal-Wallis (p-value below 0.05) were performed to detect significant differences in carbon and associated parameters between tidal/diurnal cycles (seasons) and also across diurnal and tidal rhythms (emersion around low tide during the day (LT/Day), emersion at night (LT/Night), immersion around high tide during the day (HT/Day) and immersion at night (HT/Night)) (emersion and immersion periods last during 4 and 8 hours twice per day in the Arcachon lagoon). The Dunn's post-hoc multiple comparisons' test to Kruskal-Wallis was chosen to detect significant differences among groups.

3. Results

3.1. Water pCO_2 and associated parameter temporal variations

3.1.1. At the seasonal time scale

In 2008/09 at our 2.5 meter deep (on average, hydrographic zero) subtidal creek in the Arcachon lagoon, water temperatures averaged 17.7 ± 4.2 °C over the years 2008 and 2009 and ranged between 8.9 ± 0.4 °C in January 2009 and 22.2 ± 0.6 °C in July 2008 (Table 1, Fig. 2). Water mean salinity value was 30.5 ± 3.4 with a particularly low mean value measured in January 2009 (Table 1, 23.2 ± 1.5, Fig. 3).

Bicarbonates (HCO_3^-), carbonates (CO_3^{2-}) and the sum of dissolved CO_2 and carbonic acid H_2CO_3 concentrations (CO_2^*) represented respectively 91 to 95 %, 3 to 8 % and about 1 % of the whole DIC (data not shown). TA values followed DIC patterns with a lowest mean value of 1.646 ± 0.086 mmol kg^{-1} in January 2009 and a highest mean value 2.255 ± 0.021 mmol kg^{-1} in September 2008 (Fig. 3, Table 1). δ^{13}C-DIC mean values were close to 0 ‰ and ranged between -1.1 ± 1.1 ‰ in April 2008 (minimum values in winter/spring) and -0.2 ± 0.2 ‰ in June 2009 (maximum values in summer/autumn). Particularly low negative values up to -3.7 ‰ were measured in April 2008 (Table 1, Fig. 3). Over the whole studied period, global

299 significant and positive TA, DIC and δ^{13}C-DIC values versus salinity values were obtained
300 (TA=0.05143*S + 0.5079, R^2: 0.88; DIC=0.03815*S + 0.7594, R^2: 0.82; δ^{13}C-DIC=0.08697*S
301 - 3.284, R^2: 0.15; $p<0.0001$, Fig. 4a, c, d). At each cycle (season) apparent 0 end-member TA
302 and *in situ* catchment TA values were computed from the Y-intercept of TA versus S cross-
303 correlations (Fig. 4a) and *in situ* TA measurements carried out at the same time over the
304 Arcachon lagoon watershed watercourses (Polsenaere et al. 2012b) calculated here as
305 discharge-weighted TA means, respectively (Fig. 4b). Apparent 0 end-member TA values were
306 generally higher than *in situ* catchment values except during the end of summer and autumn
307 period (September and November 2008, Fig. 4b).
308 Water pCO_2 averaged 496 ± 36 ppmv over the sampling years and were always oversaturated
309 whatever the season and period of the day and tide, with regards to the atmospheric equilibrium
310 of 390 ppmv (Figs. 2, 3, 5, Table 1). Mean values ranged from 461 ± 14 ppmv in July 2008 to
311 530 ± 39 ppmv in September 2009 (minimum and maximum values in summer/autumn) with
312 in general (except between November and July 2008 and between April and September 2009)
313 only significant differences between seasons (Kruskal-Wallis test, $p<0.05$) though lower than
314 those observed at the diurnal/tidal scale (Table 1, Figs. 2, 3, 5).
315 Seasonal variations in *in situ* measured temperature, pCO_2 values and in temperature ($TpCO_2$,
316 $tpCO_2$) versus non-temperature ($NpCO_2$) effects on pCO_2 are presented in Figure 2. During
317 2008, pCO_2 values showed weak seasonal variations increasing from April 2008 (474 ± 14
318 ppmv) to September 2008 (515 ± 36 ppmv) before decreasing towards November 2008 (463
319 ppmv). In 2009, pCO_2 increased from January to April (525 ± 14 ppmv) before decreasing
320 towards June (490 ± 27 ppmv) and increasing again to September (530 ± 39 ppmv, Table 1,
321 Fig. 2) as in 2008. In 2008, $NpCO_2$ values showed larger seasonal variations first decreasing
322 from April to July (557 ± 22 and 381 ± 16 ppmv respectively), and then increasing towards
323 November (583 ± 27 ppmv). To the contrary in 2009, a decrease was first observed from

January (698 ± 16 ppmv) to June 2009 (417 ± 24 ppmv) before increasing towards September (463± 37 ppmv). In 2008 and 2009 respectively, $TpCO_2$ followed exactly the opposite patterns. Peak-to-peak seasonal amplitudes in *in situ* temperature and pCO_2 values were 9.9 °C and 52 ppmv in 2008 and 12.6 °C and 50 ppmv in 2009 (Fig. 2, Table 1).

3.1.2. At the diurnal/tidal time scales

Significant variations in inorganic carbon and associated parameters occurred at the diurnal/tidal scales (Table 1, Figs. 2, 3, 5). Water heights ranged from 0.4 m (July 2008 and June 2009) at low tide to 4.5 m (July 2008, January and June 2009) at high tide (Fig. 3). The largest salinity variation occurred during winter and spring with for instance 5.2 and 6.7 salinity unit difference between low and high tides in January and April 2009 respectively. During these seasons, at low tide, the lowest salinity values of 20.4 and 24.8 respectively were observed. To the contrary, during summer and autumn seasons, salinity values were higher (minimum values 30.2 at low tide in July 2008 and June 2009) and varied by less than 2.4 units throughout the tidal cycle (Table 1, Figs. 3, 5). Water temperature variations at the tidal/diurnal scales were small and ranged from 1.4/1.3 °C in September 2008/2009 to 3.3 °C in June 2009 (Table 1, Figs. 3, 5).

With regards to inorganic carbon parameters, DIC and TA concentrations showed weak diurnal/tidal variations with significant differences between high and low tides except in September 2008 (ranges of 0.078 mmol $kg^{-1}$for TA and 0.069 mmol kg^{-1} for DIC) and in June 2009 where lower values were measured during low tide periods, concomitant to lower salinities. δ^{13}C-DIC values were significantly higher during high tide in July 2008 and June 2009 (ranges: -1.7 to 0.2 ‰ and -0.4 to 0.2 ‰, respectively) (Table 1, Fig. 3).

Water pCO_2 tidal/diurnal variations ranged between 50 ppmv in winter and spring (51 and 54 ppmv in January 2009 and April 2008 respectively) to 150-200 ppmv in summer and autumn (148 and 192 ppmv in September 2009 and 2008) (Figs. 2, 3, 5). Whatever the season and hour,

water pCO_2 values were always oversaturated compared to the atmospheric value of 390 ppm; at minimum over all tidal/diurnal cycles, pCO_2 value dropped to 405 ppmv in September 2008) (Table 1, Figs. 2, 3, 5). Some significant pCO_2 variations also occurred in the creek between nighttime and daytime and between the emersion and the immersion of the tidal flat (LT_D, LT_N, HT_D and HT_N periods, see Fig. 5 caption and M&M section) (Non-parametric Mann-Whitney test, $p<0.05$) (Figs. 3 and 5, Table 1). In winter-spring (April 2008, November 2008, January 2009 and April 2009), during daytime pCO_2 were significantly higher and daytime salinity were lower than at night. To the contrary, in summer-autumn (July 2008, September 2008/09 and June 2009), daytime pCO_2 values were significantly lower than nighttime pCO_2 and salinity were higher at night. During the eight cycles, pCO_2 values at low tide were significantly higher than values at high tide (salinity values at low tide were also below high tide values) (Figs. 2, 3, 5, Table 1).

A correlation analysis showed significant negative correlations between water pCO_2 and salinity (or water height) values (i.e. Spearman coefficients pCO_2 versus salinity of -0.69 and -0.92, $p<0.01$ in July 2008 and September 2009 respectively), except in September and November 2008 (Fig. 3). pCO_2 values were also negatively correlated to δ^{13}C-DIC values in July 2008 and over all 2019 cycles (R: -0.63, -0.72 and -0.58 in July 2008, January and June 2009 respectively, $p<0.01$). TA concentrations appeared to be always significantly and positively correlated to salinity (or water height) (R: 0.93 and 0.80, $p<0.01$ in September 2008 and April 2009 for instance) and to DIC concentrations (Figs. 2, 3). δ^{13}C-DIC values were significantly and positively correlated to salinity and water height (H) values in July 2008 and over all 2019 cycles (R: 0.45, 0.70 in July 2008 and April 2009 respectively, $p<0.01$), to TA values in September 2008 and over all cycles in 2019 (R: 0.46, 0.59 in September 2008 and 2009 respectively, $p<0.01$) and to DIC concentrations over all cycles in 2009 (R: 0.61 and 0.76 in April and June 2009 respectively) (Fig. 4).

3.2. Gas transfer velocities and atmospheric CO_2 fluxes from the Arcachon lagoon waters

Wind speeds (U_{10}) ranged between 2.41 ± 1.05 and 7.74 ± 1.77 m s^{-1} in September and November 2008 respectively with significant differences noticed between September 2008 - January 2009 (minimum values) and July - November 2008 - September 2009 (maximum values) (Kruskal-Wallis and Dunn's post-test, $p < 0.01$, Table 2). k_{600} values were in average estimated at 8.54 ± 6.75, 17.29 ± 15.76 and 17.00 ± 6.23 cm h^{-1} according to W92, RC01 and A09 equations respectively (see Material and Methods, Table 2). Minimum mean values occurred in September 2008 - January 2009 (1.82 ± 1.25, 4.4 ± 1.36 and 9.58 ± 3.3 cm h^{-1} in January 2009 with the three methods respectively, Table 2) whereas the highest values were reached in November 2008 - September 2009 (19.37 ± 8.37, 33.33 ± 19.51 and 28.38 ± 6.12 cm h^{-1} in November 2008 with the three methods respectively, Table 2). In April 2008 and September 2009 at high tide, k_{600} (and U_{10}) values were also found significantly different between day (higher values) and night (lower values) periods (Mann-Whitney test, $p < 0.05$) whatever used methods (Table 2).

Mean water-air CO_2 fluxes were estimated at 0.27 ± 0.22, 0.56 ± 0.54 and 0.55 ± 0.22 mmol m^{-2} h^{-1} according to W92, RC01 and A09 equations respectively (Table 2). Minimum mean values were observed in January 2009 (0.06 ± 0.04, 0.14 ± 0.06 and 0.29 ± 0.13 mmol m^{-2} h^{-1} with the three methods respectively) whereas the highest values were reached in September 2009 (0.62 ± 0.66, 1.67 ± 2.36 and 0.82 ± 0.47 mmol m^{-2} h^{-1} with the three methods respectively, Table 2). In April 2008 and September 2009, water-air CO_2 flux values were also found significantly different between day (higher values) and night (lower values) periods (Mann-Whitney test, $p < 0.05$) as it was the case for k_{600} and U_{10} values whatever used methods (Table 2). Water-air fluxes estimated from A09 equation were significantly higher than values estimated from W92 (and RC01) equations (Kruskal-Wallis and Dunn's post-test, $p < 0.01$)

except in November 2008 - April 2009 - September 2009 where no significant difference was observed between methods.

In July 2008, an atmospheric EC mast was deployed in the Arcachon lagoon simultaneously and close (at 1.8 km) to the 24 hours cycle location (Fig. 1, Table 2; Polsenaere et al. 2012a). During the whole tidal cycle in July 2008, EC fluxes averaged 0.45 ± 7.71 mmol m^{-2} h^{-1} and ranged from -17.98 to 43.19 mmol m^{-2} h^{-1}. EC water-air CO_2 fluxes during the immersion were on average -1.39 ± 2.67 mmol m^{-2} h^{-1} and ranged from -12.38 to 2.10 mmol m^{-2} h^{-1} with significantly lower values during daytime period (Mann-Whitney test, $p < 0.05$). Significant differences were computed between direct water-air CO_2 fluxes measured during the immersion at the EC site and calculated CO_2 fluxes from pCO_2 records at the channel site according to RC01 - A09 equations (Kruskal-Wallis and Dunn's post-test, $p < 0.01$; Table 2).

4. Discussion

4.1. Seasonal compensation of thermal and non-thermal effects on water pCO_2

In the Arcachon lagoon, seasonal variations in water inorganic carbon parameters and especially pCO_2 were relatively weak and on the lower range for waters influenced by an intertidal ecosystem when compared to other coastal ecosystems worldwide (Borges et al. 2005; Table 3). We observed a maximal pCO_2 variation of 196 ppmv between the lowest and the highest values measured during each 12- or 24-hour cycles and the maximum pCO_2 (averaged over each 24-hour cycle) amplitude barely reached 70 ppmv.

At the seasonal scale over coastal bays, thermal but also non-thermal effects can significantly influence water pCO_2 variations. In the studied lagoon, we observed that, seasonally, biological effects that consisted in more heterotrophy in winter and more autotrophy in summer, was offset by the thermal effect induced by the variation of water temperature (from 8.9 to 22.2 °C) resulting in relatively constant pCO_2 values throughout the year. Furthermore, other non-

423 thermal effects were induced by mixing of freshwater in the lagoon, particularly in January
424 2009 when salinity decreased down to 20.4 (Table 1, Figs. 3, 4). River waters discharging in
425 the lagoon are yearly oversaturated in CO_2 (Polsenaere et al. 2012b) and their positive influence
426 on pCO_2 values was supposed to be maximal in January 2009 (Table 1, Fig. 3). Overall, thermal
427 and non-thermal components of pCO_2 strongly varied seasonally, almost compensating each
428 other. For instance, the six months $\Delta TpCO_2$ offset (260 ppmv) observed from July 2008 to
429 January 2009 ($TpCO_2$ from 601 to 341 ppmv) concomitantly to the 13.3 °C water temperature
430 decrease (from 22.2 to 8.9 °C) barely compensated non-thermal effects on water pCO_2 that
431 occurred during that six-month period ($\Delta NpCO_2$ = 317 ppmv, from 381 to 698 ppmv) (Fig. 2).
432 In spring and summer, more autotrophic metabolism by all benthic and planktonic primary
433 producers of the lagoon is favored and less remineralization occurs resulting in the lowest
434 $NpCO_2$ values, while the effect of autotrophy on pCO_2 is offset by water heating. Phytoplankton
435 blooms occur in the lagoon especially from the spring season that shows the highest primary
436 production rates (between 231.4 and 496.6 mg C m^{-3} d^{-1} in 2003, Glé et al. 2008). Influxes of
437 CO_2 in spring and early autumn were measured on the flat by the EC station (Polsenaere et al.
438 2012a). *Zostera* seagrass meadows also contribute significantly to the total primary production
439 of the Bay (Plus et al. 2015; Polsenaere et al. 2012a; Ribaudo et al. 2017) and then may
440 influence pCO_2 dynamics as observed elsewhere in the eastern shore of Virginia by Berg et al.
441 (2019). In summer in the lagoon, higher *Zostera* seagrass net primary production associated
442 with lower heterotrophic respiration result in more autotrophic sediment metabolism; together
443 with phytoplanktonic and immersed *Zostera* production and lower freshwater inputs to the
444 lagoon explain the $NpCO_2$ drawdown from January to June 2009 (281, from 698 to 417 ppmv).
445 However, in summer, *Zostera* primary production probably occurs using mostly CO_2 directly
446 from the atmosphere during the emersion and even more if low tide is around midday
447 (Polsenaere et al. 2012a). Thus, in the studied channel the direct influence of *Zostera*

448 metabolism on water pCO_2 is probably modest. To the contrary from spring to summer-autumn
449 2009 periods, $NpCO_2$ values increased (46, from 417 to 463 ppmv) whereas primary production
450 decreased. In autumn and winter contrarily to summer season, heterotrophy is favored because
451 the seagrass biomass is recycled and decomposed in the sediments and the waters (Auby and
452 Labourg 1996). The *Zostera* meadow decline feeds the lagoon sediments and waters with
453 organic matter, favoring heterotrophy which together with a lower planktonic primary
454 production and also more freshwater inputs to the lagoon, contribute to the highest $NpCO_2$
455 values measured in November 2008 and January 2009 (Fig. 2). At the same time, this
456 combination of all factors on water pCO_2 is compensated by water cooling and in consequence,
457 a pCO_2 value seasonally constant at about 500 ppmv was measured in the lagoon. Other studies
458 showed a more pronounced effect of either thermal or non-thermal variations on water pCO_2 at
459 the seasonal scale as for instance Ribas-Ribas et al. (2011) that reported in the Bay of Cadiz
460 during winter a dominant thermal control in comparison with non-thermal effects, or to the
461 contrary, Bozec et al. (2011) who showed in the Bay of Brest, a stronger influence of non-
462 thermal (biology) processes on seasonal pCO_2 dynamics (Table 3).
463
464 **4.2. Seasonal carbonate chemistry and mixing patterns of freshwater and seawater DIC**
465 Besides biological activity and its light-temperature controlled seasonal evolution, horizontal
466 advection and exchanges between terrestrial-lagoon-oceanic waters producing different mixing
467 patterns, strongly drives observed carbonate chemistry at the seasonal scale in the lagoon.
468 Hydrodynamic forcing importance was shown in other tidal systems such as a freshwater or
469 salty marshes where intense exchanges between marsh and coastal/estuarine waters occurred
470 during hydrological floods (Neubauer and Anderson 2003, and references in Table 3). Intense
471 exchanges of oceanic and continental waters occurred within the Arcachon lagoon as well
472 through channels or over the tidal flat around high tide (Plus et al. 2009; Polsenaere et al. 2012a,

473 b). A significant influence of freshwater discharge in the lagoon occurred in winter of the year
474 2009 with the lowest salinities (20.5-24.5) associated to the lowest TA concentrations (1.493-
475 1.733 mmol kg^{-1}) measured through our tidal cycle sampling (Fig. 3e). These low values
476 especially at low tide reflected the freshwater inputs to the lagoon from rivers draining the
477 podzolized acidic catchment (Polsenaere et al. 2012b). Furthermore, in the lagoon, water
478 seasonal mean TA values were always above corresponding DIC concentrations (maximum
479 hourly measured DIC values were below minimum TA values too) except in January and April
480 2009. It highlights the seawater influence at the sampled channel station in the middle position
481 inside the lagoon where CO_3^{2-} provides the first line of buffering capacity as observed by Wang
482 et al. (2016) in the Sage Lot Pond salt marsh system. The significant positive correlations
483 between δ^{13}C-DIC values and salinity values, TA values and DIC concentrations over all 2019
484 cycles (Fig. 4a, c, d) supports the importance of alkalinity (CO_3^{2-}) among other DIC species
485 and thus an overall seasonal DIC variation control through tidal forcing.
486 Comparing apparent 0 end-member TA and *in situ* catchment TA values at each cycle (season),
487 we highlighted that alkalinity production occurred within the lagoon especially in April, July
488 2008 and September 2009 when 0 end-member TA values were at least two times higher than
489 *in situ* catchment weighted mean TA values (Fig. 4b). The Arcachon flat constitutes an
490 important stock of carbonates of about 120 Mt of several shellfish species represented at 95 %
491 by *Crassostrea gigas* (Polsenaere et al. 2012a). From the end of the reproduction season
492 (November) to the spat removing in spring, early development stages of bivalves are
493 particularly sensitive to dissolution-induced mortalities as shown by Barros et al. (2013)
494 through larval viability laboratory experiments on the Pacific oyster *Crassostrea gigas*. Thus,
495 $CaCO_3$ dissolution could occur in wet mud sediments in presence of such shellfishes patchily
496 distributed on the tidal flat. To the contrary, in late summer (September) and autumn
497 (November) 2008, *in situ* catchment TA values were slightly higher than 0 end-member TA

values supporting the possibility of calcification processes in the lagoon (Fig. 4b). Seagrass systems are recognized to be important site of high calcium carbonate ($CaCO_3$) cycling, both in terms of production and dissolution, such as *Posidonia oceanica* meadows where $CaCO_3$ precipitation can overwhelm sediment $CaCO_3$ dissolution particularly during net autotrophic periods (Barron et al. 2006). In any cases, net TA production in the lagoon remains more important in comparison with calcification at the annual scale.

4.3. Processes controlling tidal and diurnal pCO_2 and DIC variations

4.3.1. Large tidal DIC variations through current advection

Over intertidal systems as Arcachon, horizontal advection can strongly control water pCO_2 and carbonate chemistry variations at the tidal scale too. Significant negative correlations between pCO_2 and salinity or water height occurred most of the time in each season (except in Sept. and Nov. 08) and for each tidal/diurnal periods. The fact that higher pCO_2 values associated to lower salinity and depth values at low tide (opposite pattern during high tide) were systematically measured irrespective of day or night status supports the significant tidal rhythm control on water pCO_2 in the lagoon. For example, during the June 2009 cycle, pCO_2 and TA values were significantly inversely correlated and respectively negatively and positively correlated to water height, salinity and δ^{13}C-DIC values. Significantly higher TA concentrations associated to higher δ^{13}C-DIC values (typical oceanic TA and δ^{13}C-DIC values) were also measured during high tide periods contrarily to pCO_2 values (Table 1, Fig. 3). These results clearly reflected tidal forcing on carbonate chemistry through ocean exchange with more buffered waters on one hand and riverine inputs with more acidic waters on the other hand. In the Arcachon lagoon, maximum pCO_2 values measured at low tide were well below those measured over other coastal systems as tidal flats nearby and small marsh-estuary or mangrove tidal creeks further (Table 3). A 24 hour-cycle performed in May 2006 (not shown) in a shallower creek close to the outlet

523 of a small river North East in the back of the Arcachon lagoon showed the highest pCO_2 values
524 (up to 1300 ppmv, salinity values close to 28) at mid-ebb when the tidal flat was still immersed
525 compared to the low tide period, when the flat was emerged and the channel connected to the
526 river, with associated decreased and lower pCO_2 and salinity values (close to 800 ppmv and
527 22-23, respectively, data not shown). Thus, these measurements suggest another associated
528 process (i.e. tidal pumping, see next 4.3.2. discussion part) along with freshwater mixing that
529 occur together in the Arcachon flat.
530
531 ***4.3.2. Tidal porewater pumping and associated water alkalinity production and pCO_2***
532 ***variations***
533 During tidal cycles conducted at the channel station, TA (or DIC) concentrations showed
534 overall weak tidal variations (Fig. 3). Porewater pumping over tidal coastal vegetated
535 ecosystems (seagrass meadows, salt marshes and mangroves) has been recognized as an
536 important process in water DIC production (Neubauer and Anderson 2003; Wang et al. 2016;
537 Borges et al. 2003; Maher et al. 2013). Indeed, high alkalinity values can be reached through
538 aerobic respiration coupled to carbonate dissolution but also through organic matter anaerobic
539 remineralization products, i.e. N_2 from net denitrification and reduced sulfur (pyrite burial)
540 from net sulfate reduction (Hu and Cai 2011). In Arcachon, tidal pumping has been highlighted
541 as a significant process controlling benthic phosphorus and iron cycles over seagrasses where
542 below the rhizosphere, Fe(II) can be exposed to a reduced environment and precipitates as FeS
543 and pyrite (Deborde et al. 2008b). De Wit (2008) showed the importance of sulfate-reducing
544 bacteria in *Zostera* seagrass sediments at a tidal flat station very close to our 24-hour cycle
545 station. Moreover, Heijs et al. (1999) showed at the same location that a substantial population
546 of aerobic sulfide-oxidizing bacteria was also present, buffering free sulfide through chemical
547 processes with iron leading to high FeS and pyrite concentrations in sediments. In particular,

548 sulfide oxidation (depending on whether sulfide will be oxidized to sulfate or to sulfur) was
549 estimated at 4694 x 10^3 or 1174 x 10^3 mol cm^{-3} day^{-1}, whereas previously measured sulfate
550 reduction rates at the same station ranged from 150 to 1300 nmol cm^{-3} day^{-1}. These findings
551 along with the quantitative apparent 0 end-member and *in situ* catchment TA value (Fig. 4b)
552 suggest a substantial TA production though tidal porewater pumping along the year. Its
553 influence on TA (or DIC) production in the lagoon could not be clearly seen from our chosen
554 site, which have high salinities and TA values, hiding the terrestrial influence and did not cover
555 the 0 end-member. In any cases, in Arcachon, alkalinity production through tidal pumping is
556 not so strong in comparison with other mentioned mangrove or saltmarsh systems. Maher et al.
557 (2013) measured in a small tidal mangrove creek (Australia) during summer and winter a clear
558 tidal trend for DIC as in the present study (highest and lowest values reached during low and
559 high tides, respectively). However, a 0.736 mmol kg^{-1} DIC range (between 2.064 and 2.8 mmol
560 kg^{-1}) was measured there when in the Arcachon channel we only measured a tidal DIC variation
561 of 0.216 mmol kg^{-1} (April 2009) at maximum (0.116 mmol kg^{-1} in average over the whole study
562 period). In the Sage Lot Pond tidal marsh, Wang et al. (2016) measured in Summer tidal TA
563 variation ranges close to 0.4 mmol kg^{-1} respectively when at Arcachon a variation of 0.261
564 mmol kg^{-1} at maximum (0.133 mmol kg^{-1} in average) was seen. Similarly, according to tidal
565 pCO_2 variations, smaller variations were measured in comparison to other salt marsh-estuary
566 or mangrove creek systems, where stronger tidal pCO_2 variations were observed according to
567 porewater mixing (Table 3).
568
569 ***4.3.3 Significant diurnal pCO_2 patterns linked to biological activity***
570 In subtidal coastal ecosystems, pelagic and benthic biological activities can generate large
571 diurnal water pCO_2 variations. Indeed, in comparison with Arcachon, similar and even higher
572 diurnal pCO_2 ranges were measured in macrophyte meadows (Baltic Sea, Florida and Virginia)

573 or in bay channels (Spain) (Table 3). However, in these subtidal ecosystems, tidal pumping was
574 supposed to be minor; in the Arcachon lagoon, pCO_2 variations occur at the tidal scale through
575 porewater pumping and water masses mixing, these latter being superposed on those occurring
576 at the diurnal scale and linked to solar radiation and light availability.
577 During all sampled cycles, no significant pCO_2 versus Chl-*a* concentration relationships were
578 computed and Chl-*a* concentrations never reached more than 1.9 µg L^{-1} in average (data not
579 shown). Our successive tidal/diurnal cycle samplings in the central lagoon channel were
580 apparently not able to fully catch these blooms especially in spring and summer. However,
581 interesting diurnal pCO_2 patterns related to biological activity could be detected when
582 comparing nighttime with daytime values for a same salinity range. For instance, in September
583 2008, at low tide in the channel for a salinity range values close to 33, lower water pCO_2 and
584 higher temperature values were measured at daytime (400-525 ppmv, > 20 °C) than at nighttime
585 (550-600 ppmv, close to 19 °C) (Fig. 5e, f). The same pattern was observed in June 2009 as
586 well (Fig. 5m, n). Phytoplankton possibly with resuspended microphytobenthos communities
587 in the channel then appeared to be active at that moment. Savelli et al. (2019) showed precisely
588 that almost half (43 %) of MPB primary production can be resuspended annually over intertidal
589 lagoons and the highest occurs in spring tide at the flood beginning due to high current
590 velocities and low water heights. To the contrary, in April 2009 during flooding, water pCO_2
591 (500-560 ppmv) increased (while S increased and T decreased) whereas during ebbing, water
592 pCO_2 (538-494 ppmv) decreased and was lower (while S decreased and T increased) (Fig. 5k,
593 l). At that particular moment in the channel, organic matter produced by primary production
594 could feed community respiration through incoming coastal waters during flooding. The
595 significant negative correlation computed between pCO_2 and $\delta^{13}C$-DIC values is consistent
596 with an organic matter mineralization process that occurred in spring in the lagoon.

To assess the biological control on measured pCO_2 patterns in the studied channel, we statistically compared, when possible, night and day pCO_2 values averaged over the same salinity range (i.e. with no significant salinity value difference between day and night periods) according to tide phases for each cycle (Table 4). During flooding, daytime pCO_2 were significantly lower than those nighttime pCO_2 values and to the contrary, during ebbing phase, daytime pCO_2 were significantly higher night time pCO_2 values. At the same time, significant variations in water temperature between day and night times for both flooding and ebbing periods occurred. Water temperature gradients exist and could influence diurnal pCO_2 variations. However, they cannot alone explain these variations at our sampling station since differences between the theoretical pCO_2 variations due to diel temperature differences and measured changes in water pCO_2 for the same salinity range are large (Table 4).

Overall, these reproductible patterns strongly support the control of pCO_2 by biological activity (primary production of phytoplankton, MPB and seagrasses). Koné et al. (2009) reported pCO_2-oversaturated waters in some lagoons of Ivory Coast (West Africa) behaving as macrotidal estuaries due to net ecosystem heterotrophy and riverine CO_2 rich water inputs. To the contrary pCO_2-undersaturated waters were found in the other lagoons showing permanent hyaline stratification leading to higher phytoplankton biomass. In other systems such as Tampa and Florida bays, pCO_2 diurnal variability was mostly influenced by biological processes such as photosynthesis/respiration of benthic communities and precipitation/dissolution of calcium carbonate respectively (Table 3). Interestingly and contrary to other studied salt marsh and mangrove systems (Table 3) where tidal pumping is predominant, water pCO_2 and DIC variations in the Arcachon lagoon seemed to result from the subtle combination of thermal, water column primary production, and tidal pumping effects along with thermodynamic mixing between seawater and freshwater.

622 **4.4. High heterogeneity in water-air CO_2 fluxes over the Arcachon lagoon**

623 ***4.4.1. Turbulence forcing control on water-air CO_2 flux temporal variability***

624 The subsurface waters of the Arcachon lagoon remained always oversaturated and close to the
625 atmospheric equilibrium at both seasonal and diurnal scales. Annual mean air-sea CO_2 fluxes
626 were estimated at 0.27 ± 0.22, 0.56 ± 0.54 and 0.55 ± 0.22 mmol m^{-2} h^{-1} depending on the gas
627 transfer velocity-wind parameterizations. Water-air CO_2 flux values remained in the lower
628 range of annual values reported for macrotidal estuaries (0.58-8.42 mmol m^{-2} h^{-1}) (Borges et al.
629 2005). Similar intertidal systems showed different values with more variations at both diurnal
630 and seasonal scales (Table 3). In other subtidal and marine systems, fluctuations between CO_2
631 sink and source could also be measured over the year depending on seasons (Table 3).
632 In the Arcachon lagoon, wind speed influence on calculated air-sea CO_2 fluxes was significant
633 and could be more important in determining the intensity of the flux, than the pCO_2 air-sea
634 gradient itself. Despite significant pCO_2 variations generally noticed at seasonal and
635 tidal/diurnal scales, only few significant air-sea CO_2 flux differences were observed (i.e.
636 between November and September 2008 and between September 2008 and 2009),
637 concomitantly to significant differences in U_{10} and K_{600} values (Table 2). Thus, air-sea CO_2
638 flux variability in the Arcachon lagoon at all temporal scales appears to be controlled by
639 turbulence (K_{600}, physical forcing) rather than air-water pCO_2 gradients. This finding is the
640 opposite of what it is generally observed over dynamic coastal bays at temperate and tropical
641 latitudes characterized by higher diurnal/tidal water pCO_2 gradients (Table 3).
642
643 ***4.4.2. High heterogeneity in water-air CO_2 fluxes according to space and methodology***
644 CO_2 fluxes were estimated at the water-air interface based on k_{600} parameterizations from
645 Wanninkhof et al. (1992), Raymond and Cole (2001) and Abril et al. (2009). These
646 parameterizations were obtained over oceanic and estuarine systems with different approaches,

647 i.e. the bomb ^{14}C inventory in the ocean, non-intrusive tracer data and chamber measurements
648 respectively. The Abril et al. (2009) relationship gave significantly higher flux values compared
649 to the two others, potentially due to bottom current contributions from 2 to 20 cm s^{-1} according
650 to seasons and associated hydrodynamic modelling estimations. In July of the year 2008,
651 significant differences were computed between simultaneous direct EC fluxes and estimated
652 fluxes from gas transfer parameterizations (Table 2). No k_{600} calculations or flux data
653 comparisons were attempted from these simultaneous EC flux and water pCO_2 measurements
654 due to strong spatial heterogeneity in water bodies (separated from 1.8 km) highlighted in the
655 present study and due to the strong variability in gas transfer velocity and CO_2 flux calculations
656 according to methodologies too (Polsenaere et al. 2012a; Raymond and Cole 2001; Vachon et
657 al. 2010).
658 Indeed, variability in water pCO_2 and air-sea CO_2 fluxes depends on site locations inside a same
659 coastal ecosystem at the different temporal scales. The spring 2006 cycle carried out in the back
660 of the Arcachon lagoon (4.3.1. discussion part) showed higher water pCO_2 tidal variations (680-
661 1330 ppmv) and resulted in a higher CO_2 source to the atmosphere at this more terrestrial
662 influenced location. These observations suggest that large differences in water pCO_2 and sea-
663 air CO_2 fluxes could occur at smaller spatial scale due to specific processes and characteristics
664 that exist at the sampled area. In the lagoon, benthic primary producers such as *Zostera noltei*
665 seagrass meadows and resuspended microphytobenthic communities could influence in a
666 different way carbon dynamics and air-sea fluxes at the channel station sampled here, compared
667 to swallow waters above the tidal flat as revealed by EC measurements (Polsenaere et al.
668 2012a). Indeed, a CO_2 influx was detected during the emersion by the EC, but we never
669 observed CO_2 undersaturated waters in the channel during the July 2008 cycle. Due to the
670 strong influence of tidal advection on water pCO_2 in the intertidal lagoon, water masses sampled
671 at the studied station were not the same as those caught in the EC footprint during in July 2008

672 (Tables 1 and 2, Polsenaere et al. 2012a). This could also explain the significant differences in
673 air-sea CO_2 fluxes and associated gas transfer velocities we got from both methodologies, and
674 methodological and logistical complexity to get concomitant water-air EC flux and equilibrator
675 water pCO_2 values from the same water mass in the lagoon. Wang et al. (2018) over the Duplin
676 River salt marsh-estuary (Georgia), though different from Arcachon due to the most of the time
677 emersion canopy (ecosystem-atmosphere flux there versus water-atmosphere flux based on
678 water pCO_2 here) specifically suggested EC measurements of salt marsh net ecosystem
679 exchange could underestimate net ecosystem production for not accounting for lateral DIC
680 exchanges with tidal inundation.
681
682 **Conclusions**
683 Waters of the Arcachon lagoon represents a permanent weak CO_2 supersaturation characterized
684 by a seasonal compensation of thermal and biological effects and carbonate chemistry and
685 mixing patterns of freshwater and seawater DIC. At smaller time scales if large tidal DIC
686 variations through current advection were observed, weak tidal porewater pumping and
687 associated water alkalinity production and pCO_2 variations were noticed compared to other
688 tidal creeks surrounded by mangrove or saltmarshes. Accurate water monitoring such as that
689 carried out in this study permits high resolution analysis of the carbon signal; small but
690 significant pCO_2 variations were seen at the diurnal scale (between 5 and 24 ppmv) linked to
691 the light cycle apparently induced by planktonic and benthic productivity in the channel along
692 to day versus night temperature gradients at flooding and ebbing periods. The temporal
693 variability and the high heterogeneity in computed water-air CO_2 fluxes according to space
694 (water masses) and methodology (EC, …) would require more integrated carbon fluxes and
695 processes over tidal ecosystems as here for the Arcachon lagoon.
696

Acknowledgments

We would like to express our thanks to Francis Prince the Planula boat captain. This paper is a contribution to the PNEC (Programme National Environnement Côtier)-Littoral Atlantique and ANR PROTIDAL (Agence Nationale de la Recherche « Processus biogéochimiques transitoires de la zone intertidale ») projects.

Competing Interests

The authors declare no competing interests.

References

Abril, G., M. Commarieu, A. Sottolichio, P. Bretel, and F. Guérin. 2009. Turbidity limits gas exchange in a large macrotidal estuary. *Estuarine, Coastal and Shelf Science* 83: 342–348.

Abril, G., Deborde, J., Savoye, N., Mathieu, F., Moreira-Turcq, P., Artigas, F., Meziane, T., Takiyama, L. R., de Souza, M. S., Seyler, P. 2013. Export of ^{13}C-depleted dissolved inorganic carbon from a tidal forest bordering the Amazon estuary. *Estuarine, Coastal and Shelf Science*, 129: 23-27.

Amanieu, M. 1967. Recherches écologiques sur la faune des plages abritées et des étangs saumâtres de la région d'Arcachon. *PhD Thesis, Université Bordeaux 1*, pp. 234.

Amorocho, J. and J.J. DeVries. 1980. A new evalution of the wind stress coefficient over water surfaces. *Journal of Geophysical Research* 85: 433–442.

Auby, I., F. Manaud, D. Maurer, and G. Trut. 1994. Étude de la prolifération des algues vertes dans le bassin d'Arcachon. *Report Prepared by IFREMER, Arcachon, France, for CEMAGREF-SSA-SABARC*, pp. 1–163.

721 Auby, I. and P.J. Labourg. 1996. Seasonal dynamics of *Zostera noltii* Hornem. in Bay of
722 Arcachon (France). *Journal of Sea Research* 35: 269–277.
723 Barron, C., C. M. Duarte, M. Frankignoulle, and A.V. Borges. 2006. Organic carbon
724 metabolism and carbonate dynamics in a Mediterranean seagrass (*Posidonia oceanica*)
725 meadow. *Estuaries and Coasts* 29: 417–426.
726 Barros, P., P. Sobral, P. Range, L. Chícharo, and D. Matias. 2013. Effects of sea-water
727 acidification on fertilization and larval development of the oyster *Crassostrea gigas*.
728 *Journal of Experimental Marine Biology and Ecology* 440: 200–206.
729 https://doi.org/10.1016/j.jembe.2012.12.014.
730 Bauer, J.E., W.-J. Cai, P.A. Raymond, T.S. Bianchi, C.S. Hopkinson, and P.A.G. Regnier.
731 2013. The changing carbon cycle of the coastal ocean. *Nature* 504 (7478): 61–70.
732 Berg, P., M.L. Delgard, P. Polsenaere, K.J. McGlathery, S.C. Doney S.C., and A.C. Berger.
733 2019. Dynamics of benthic metabolism, O_2, and pCO_2 in a temperate seagrass meadow.
734 *Limnology and Oceanography* 64: 2586–2604.
735 Borges, A.V. and M. Frankignoulle. 1999. Daily and seasonal variations of the partial pressure
736 of CO_2 in surface seawater along Belgian and southern Dutch coastal areas. *Journal of*
737 *Marine Systems* 19 (4): 251–266.
738 Borges, A. V., S. Djenidi, G. Lacroix, J. Théate, B. Delille, and M. Frankignoulle. 2003.
739 Atmospheric CO_2 flux from mangrove surrounding waters. *Geophysical Research Letters*
740 30(11), 1558. https://doi.org/10.1029/2003GL017143.
741 Borges, A. V., B. Delille, and M. Frankignoulle. 2005. Budgeting sinks and sources of CO_2 in
742 the coastal ocean: diversity of ecosystems counts. *Geophysical Research Letters* 32:
743 LI4601. https://doi:10.1029/2005GL023053.

744 Borges, A.V. and G. Abril. 2011. Carbon dioxide and methane dynamics in estuaries.
745 In *Treatise on estuarine and coastal science*, ed. E. Wolanski and D.S. McLusky 5: 119–
746 161.
747 Bouillon, S., Middelburg, J.J., Dehairs, F., Borges, A.V., Abril, G., Flindt, M.R., Ulomi, S.,
748 Kristensen, E. 2007. Importance of intertidal sediment processes and porewater exchange
749 on the water column biogeochemistry in a pristine mangrove creek (Ras Dege, Tanzania).
750 *Biogeosciences 4* (3): 311–322.
751 Bozec, Y., L. Merlivat, A.-C. Baudoux, L. Beaumont, S. Blain, E. Bucciarelli, T. Danguy, E.
752 Grossteffan, A. Guillot, and J. Guillou. 2011. Diurnal to inter-annual dynamics of pCO_2
753 recorded by a CARIOCA sensor in a temperate coastal ecosystem (2003–2009). *Marine*
754 *Chemistry* 126: 13–26.
755 Burgos, M., T. Ortega, and J. Forja. 2018. Carbon Dioxide and Methane Dynamics in Three
756 Coastal Systems of Cadiz Bay (SW Spain). *Estuaries and Coasts* 41: 1069–1088.
757 https://doi.org/10.1007/s12237-017-0330-2.
758 Cai, W.J., L.R. Pomeroy, M.A. Moran, and Y. Wang. 1999. Oxygen and carbon dioxide mass
759 balance for the estuarine-intertidal marsh complex of five rivers in the southeastern US.
760 *Limnology and Oceanography* 44: 639–649.
761 Cai, W.-J. 2011. Estuarine and coastal ocean carbon paradox: CO_2 sinks or sites of terrestrial
762 carbon incineration? *Annual Review of Marine Science* 3 (1): 123–145.
763 Canton, M, P. Anschutz, A. Coynel, P. Polsenaere, I. Auby, and D. Poirier. 2012. Nutrient
764 export to an Eastern Atlantic coastal zone: first modeling and nitrogen mass balance.
765 *Biogeochemistry* 107: 361–377.
766 Caumette, P., J. Castel, and Herbert R. 1996. Coastal Lagoon Eutrophication and ANaerobic
767 Processes (C.L.E.AN.): Nitrogen and Sulfur Cycles and Population Dynamics in Coastal

768 Lagoons. *A Research Programme of the Environment Programme of the EC (DG XII)*.
769 https://doi.org/10.1007/978-94-009-1744-6.
770 Chen, C.-T.A., Huang, T.-H., Chen, Y.-C., Bai, Y., He, X., Kang, Y. 2013. Air–sea exchanges
771 of CO_2 in the world's coastal seas. *Biogeosciences* 10, 6509–6544.
772 https://doi.org/10.5194/bg-10-6509-2013.
773 Cognat, M., F. Ganthy, I. Auby, F. Barraquand, L. Rigouin, and A. Sottolichio,
774 2018. Environmental factors controlling biomass development of seagrass meadows of
775 *Zostera noltei* after a drastic decline (Arcachon Bay, France). *Journal Of Sea Research*
776 140: 87–104.
777 Coignot, E., P. Polsenaere, P. Soletchnik, O. Le Moine, P. Souchu, E. Joyeux, Y. Le Roy, J.-P.
778 Guéret, L. Froud, R. Gallais, E. Chourré, and L.Chaigneau. 2020. Variabilité spatio-
779 temporelle des nutriments et du carbone et flux associés le long d'un continuum terrestre-
780 aquatique tempéré (Marais poitevin – Baie de l'Aiguillon – Pertuis Breton). Rapport final
781 (suivi 2017-2018) - Projet Aiguillon (2016-2020).
782 111pp. https://archimer.ifremer.fr/doc/00618/73003/
783 Cole, J.J., Y.T. Prairie, N.F. Caraco, W.H. Mcdowell, L.J. Tranvik, R.G. Striegl, C.M. Duarte,
784 P. Kortelainen, J.A. Downing, J. Middleburg, and J. Melack. 2007. Plumbing the global
785 carbon cycle: integrating inland waters into the terrestrial carbon budget. *Ecosystems* 10:
786 171–184.
787 Cotovicz, L.C., B.A. Knoppers, N. Brandini, S.J. Costa Santos, and G. Abril. 2015. A large
788 CO_2 sink enhanced by eutrophication in a tropical coastal embayment (Guanabara Bay,
789 Rio de Janeiro, Brazil). *Biogeosciences* 12: 6125–6146. https://doi.org/10.5194/bg-12-
790 6125-2015.
791 Cotovicz, L.C., B.G.Libardoni, N.Brandini, B.A. Knoppers and G. Abril. 2016. Comparações
792 entre medições em tempo real da pCO_2 aquática com estimativas indiretas em dois

793 estuários tropicais contrastantes: o estuário eutrofizado da baía de Guanabara (RJ) e o
794 estuário oligotrofico do rio São Francisco (AL). *Química Nova*. 39: 1206–1214.
795 https://doi.org/10.21577/0100-4042.20160145.
796 Dai, M., Z. Lu, W. Zhai, B. Chen, Z. Cao, K. Zhou, W. J. Cai, and C. T. A. Chen. 2009. Diurnal
797 variations of surface seawater pCO_2 in contrasting coastal environments. *Limnology and*
798 *Oceanography* 54: 735–745.
799 Deborde, J., P. Anschutz, I. Auby, C. Glé, M.V. Commarieu, D. Maurer, P. Lecroart, G. Abril.
800 2008a. Role of the tidal pumping on nutrient cycling in a temperate lagoon (Arcachon
801 Bay, France). *Marine Chemistry* 109: 98–114.
802 Deborde J., G. Abril, A. Mouret, D. Jezequel, G. Thouzeau, J. Clavier, G.
803 Bachelet, P. Anschutz. 2008b. Impacts of seasonal dynamics impact of a *Zostera*
804 *noltii* meadow on phosphorus and iron cycles in a tidal mudflat (Arcachon Bay,
805 France), *Marine Ecology Progress Series* 355, 59–71.
806 Delgard, M. L., B. Deflandre, J. Deborde, M. Richard, C. Charbonnier, and P. Anschutz. 2013.
807 Changes in Nutrient Biogeochemistry in Response to the Regression of *Zostera noltii*
808 Meadows in the Arcachon Bay (France). *Aquatic Geochemistry* 19: 241–259.
809 doi:10.1007/s10498-013-9192-9
810 Delille, B, AV Borges, and D. Delille. 2009. Influence of giant kelp beds (*Macrocystis pyrifera*)
811 on diel cycles of pCO_2 and DIC in the sub-Antarctic coastal area. *Estuarine Coastal and*
812 *Shelf Science* 81: 114–122.
813 De Wit, R. 2008. Microbial diversity in the Bassin d'Arcachon coastal lagoon (SW France).
814 *Hydrobiologia* 611: 5–15. https://doi.org/10.1007/s10750-008-9461-6.
815 Dickson, A.G. and F.J. Millero. 1987. A comparison of the equilibrium constants for the
816 dissociation of carbonic acid in seawater media. *Deep-Sea Research* 34: 1733–1743.

817 Dickson, A.G. 1990. Standard potential of the reaction: AgCl(s) + 1⁄2H2(g) = Ag(s) + HCl(aq),
818 and the standard acidity constant of the ion HSO_4^- in synthetic sea water from 273.15 to
819 318.15 K. *Journal of Chemical Thermodynamics* 22: 113–127.
820 Fauvelle, V., A. Belles, H. Budzinski, N. Mazzella, and M. Plus . 2018. Simulated conservative
821 tracer as a proxy for S-metolachlor concentration predictions compared to POCIS
822 measurements in Arcachon Bay. *Marine Pollution Bulletin* 133: 423–
823 427. https://doi.org/10.1016/j.marpolbul.2018.06.005.
824 Frankignoulle, M., I. Bourge, C. Canon, and P. Dauby. 1996. Distribution of surface seawater
825 partial CO_2 pressure in the English Channel and in the Southern Bight of the North Sea.
826 *Continental Shelf Research* 16: 381–395.
827 Frankignoulle, M., G. Abril, A.V. Borges I. Bourge, C. Canon, B. Delille, E. Libert, and J.M.
828 Théate. 1998. Carbon dioxide emission from European estuaries. *Science* 282: 434–436.
829 Frankignoulle, M, A.V. Borges, and R. Biondo. 2001. A new design of equilibrator to monitor
830 carbon dioxide in highly dynamic and turbid environments. *Water Research* 35: 344–
831 1347.
832 Ganthy, F., A. Sottolichio, R. Verney. 2013. Seasonal modification of tidal flat sediment
833 dynamics by seagrass meadows of Zostera noltii (Bassin d'Arcachon, France). *Journal*
834 *Of Marine Systems* 109: 233–240. https://doi.org/10.1016/j.jmarsys.2011.11.027.
835 Gattuso, J.-P., M. Frankignoulle, and R. Wollast. 1998. Carbon and carbonate metabolism in
836 coastal aquatic systems. *Annual Review Ecology Systematics* 29, 405–433.
837 Gazeau, F., V.S. Smith, B. Gentili, M. Frankignulle, and J.P. Gattuso. 2004. The European
838 coastal zone: characterization and first assessment of ecosystem metabolism, *Estuarine,*
839 *Coastal and Shelf Science* 60: 673–694.
840 Gillikin, D.P. and S. Bouillon. 2007. Determination of $\delta^{18}O$ of water and $\delta^{13}C$ of dissolved
841 inorganic carbon using a simple modification of an elemental analyzer—isotope ratio

842 mass spectrometer EA-IRMS: an evaluation. *Rapid Communication in Mass*
843 *Spectrometry* 21: 1475–1478
844 Glé, C., Y. Del Amo, B. Sautour, P. Laborde, and P. Chardy. 2008. Variability of nutrients and
845 phytoplankton primary production in a shallow macrotidal coastal ecosystem (Arcachon
846 Bay, France), *Estuarine, Coastal and Shelf Science* 76 (3): 642–656.
847 Gran, G. 1952. Determination of the equivalence point in potentiometric titrations. Part II.
848 *Analyst* 77: 661–671.
849 Heijs, S.K., H.M. Jonkers, H. van Gemerden, B.E.M. Schaub, and L.J. Stal. 1999. The
850 Buffering Capacity Towards Free Sulfide in Sediments of a Coastal Lagoon (Bassin
851 d'Arcachon, France) the Relative Importance of Chemical and Biological Processes.
852 *Estuarine, Coastal and Shelf Science* 49 (1): 21–35.
853 https://doi.org/10.1006/ecss.1999.0482.
854 Hu, X., and W.-J. Cai. 2011. An assessment of ocean margin anaerobic processes on oceanic
855 alkalinity budget. *Global Biogeochemical Cycles* 25: GB3003.
856 https://doi.org/10.1029/2010GB003859.
857 Jähne, B., K.O. Münnich, R. Bösinger, A. Dutzi, W. Huber, and P. Libner. 1987. On the
858 parameters influencing air-water gas exchange. *Journal of Geophysical Research* 92*:*
859 1937-1949.
860 Kjerfve, B. 1985. Comparative oceanography of coastal lagoons. *In Estuarine variability, ed.*
861 *D.A. Wolfe, New York Academic*, 63–81.
862 Koné, Y.J., G. Abril, K.N. Kouadio, B. Delille, and A.V. Borges. 2009. Seasonal variability of
863 carbon dioxide in the rivers and lagoons of Ivory Coast (West Africa). *Estuaries and*
864 *Coasts* 32: 246–260.
865 Laruelle, G. G, H. H. Durr, C. P. Slomp, and A. V. Borges. 2010. Evaluation of sinks and
866 sources of CO_2 in the global coastal ocean using a spatially-explicit typology of estuaries

867 and continental shelves. *Geophysical Research Letters* 37, L15607.
868 https://doi.org/10.1029/2010GL043691.
869 Lazure, P., and F. Dumas. 2008. An external-internal mode coupling for a 3D hydrodynamical
870 model for applications at regional scale (MARS). *Advances in water Resources* 31: 233–
871 250. http://doi.org/10.1016/j.advwatres.2007.06.010.
872 Lee, K., T.W. Kim, R.H. Byrne, F. J. Millero, R. A. Feely, and Y.M. Liu. 2010. The universal
873 ratio of boron to chlorinity for the North Pacific and North Atlantic oceans. *Geochimica*
874 *et Cosmochimica Acta* 74: 1801–1811.
875 Lewis, E. and D. Wallace. 1998. Program developed for CO_2 system calculations. *Carbon*
876 *dioxide information analysis center. Oak Ridge National Laboratory*.
877 Maher, D.T., I.R., Santos, L. Golsby-Smith, J. Gleeson, and B.D. Eyre. 2013. Groundwater-
878 derived dissolved inorganic and organic carbon exports from a mangrove tidal creek: The
879 missing mangrove carbon sink? *Limnology and Oceanography* 58: 1801–1811.
880 https://doi.org/10.4319/lo.2013.58.2.0475.
881 Mantoura, R. F. C., J. M. Martin, and R. Wollast. 1991. Ocean margin processes. *In Global*
882 *Change, Chichester, UK: Wiley & Sons*, pp. 469.
883 Mehrbach C, C.H. Culberson, J.E. Hawley, and R.N. Pytkowicz. 1973. Measurement of the
884 apparent dissociation constants of carbonic acid in seawater at atmospheric pressure.
885 *Limnology and Oceanography* 18: 897–907.
886 Migné, A., D. Davoult, N. Spilmont, V. Ouisse, and G. Boucher. 2016. Spatial and temporal
887 variability of CO_2 fluxes at the sediment–air interface in a tidal flat of a temperate lagoon
888 (Arcachon Bay, France). *Journal of Sea Research*, 109: 13-19.
889 https://doi.org/10.1016/j.seares.2016.01.003.

Miyajima, T., Y. Yamada, Y.T. Hanba, K. Yoshii, T. Koitabashi, and E. Wada. 1995. Determining the stable isotope ratio of total dissolved inorganic carbon in lake water by GC/C/IRMS. *Limnology and Oceanography* 40: 994–1000.

Mook W. G., Koopmans M., Carter A. F., and Keeling C. D. 1983. Seasonal, latitudinal, and secular variations in the abundance and isotopic ratios of atmospheric carbon dioxide. 1. Results from land stations. *Journal of Geophysical Research* 88: 10915–10933.

Neubauer, S. C. and I. C. Anderson. 2003. Transport of dissolved inorganic carbon from a tidal freshwater marsh to the York River estuary. *Limnology and Oceanography* 48: 299–307. https://doi.org/10.4319/lo.2003.48.1.0299.

Parker S. R., Poulson S. R., Gammons C. H., and Degrandpre M. D. 2005. Biogeochemical controls on diel cycling of stable isotopes of dissolved O_2 and dissolved inorganic carbon in the Big Hole River, Montana. *Environmental Science Technology* 39: 7134–7140.

Pernetta, J.C. and J.D. Milliman. 1995. Land-Ocean interactions in the coastal zone. *Implementation plan, IGPB Rep.* 33: 1–215.

Plus, M., F. Dumas, J-Y. Stanisière, and D. Maurer. 2009. Hydrodynamic characterization of the Arcachon Bay, using model-derived descriptors. *Continental Shelf Research* 29(8): 1008-1013. https://doi.org/10.1016/j.csr.2008.12.016.

Plus, M., S. Dalloyau, G. Trut, I. Auby, X. de Montaudouin, E. Emery, C. Noel, and C. Viala 2010. Long-term evolution (1988–2008) of *Zostera* spp. Meadows in Arcachon bay (Bay of Biscay). *Estuarine, Coastal and Shelf Science* 87: 357–366.

Plus, M., I. Auby, D. Maurer, G. Trut, Y. Del Amo, F. Dumas, B. Thouvenin. 2015. Phytoplankton versus macrophyte contribution to primary production and biogeochemical cycles of a coastal mesotidal system. A modelling approach. *Estuarine Coastal and Shelf Science* 165: 52–60.

914 Polsenaere P., E. Lamaud, J.-M. Bonnefond, V. Lafon, P. Bretel, B. Delille, J. Deborde, D.
915 Loustau, and G. Abril. 2012a. Spatial and temporal CO_2 exchanges measured by Eddy
916 Covariance over a temperate intertidal flat and their relationships to net ecosystem
917 production. *Biogeosciences* 9: 249-268.
918 Polsenaere, P. and G. Abril. 2012. Modelling CO_2 degassing from small acidic rivers using
919 water pCO_2, DIC and δ^{13}C-DIC data. *Geochimica et Cosmochimica Acta* 91: 220-239.
920 Polsenaere P., N. Savoye H. Etcheber M. Canton D. Poirier, S. Bouillon and G. Abril. 2012b.
921 Export and degassing of terrestrial carbon through watercourses draining a temperate
922 podzolized catchment. *Aquatic Sciences*. https://doi.org/10.1007/s00027-012-0275-2.
923 Polsenaere P., R. Lannuzel, S. Guesdon, O. Le Moine, and P. Soletchnik. 2018. Variabilité
924 spatio-temporelle des nutriments et du carbone et flux associés le long d'un continuum
925 terrestre-aquatique tempéré (Marais poitevin - Baie de l'Aiguillon - Pertuis Breton).
926 PROJET AIGUILLON (2016-2020). Rapport scientifique. 85
927 pp. *https://archimer.ifremer.fr/doc/00461/57284/*
928 Raymond, P. A. and J. J. Cole. 2001. Gas exchange in rivers and estuaries: choosing a gas
929 transfer velocity. *Estuaries* 24: 312–317.
930 Ribas-Ribas, M., A. Gómez-Parra, and J.M. Forja. 2011. Air–sea CO_2 fluxes in the north-
931 eastern shelf of the Gulf of Cádiz (southwest Iberian Peninsula). *Marine Chemistry* 123:
932 56–66. https://doi.org/10.1016/j.marchem.2010.09.005.
933 Ribas-Ribas, M., E. Anfuso, A. Gómez-Parra, and J.M. Forja. 2013. Tidal and seasonal carbon
934 and nutrient dynamics of the Guadalquivir estuary and the Bay of Cádiz (SW Iberian
935 Peninsula). *Biogeosciences* 10: 4481–4491.
936 Ribaudo C., V. Bertrin G. Jan, P. Anschutz, and G. Abril. 2017. Benthic production, respiration,
937 and methane oxydation in *Lobelia dormanna* lawns. *Hydrobiologia* 784: 21–34.
938 https://doi.org/10.1007/s10750-016-2848-x.

939 Rigaud S., B. Deflandre, O. Maire, G. Bernard, and P. Anschutz. 2018. Transient
940 biogeochemistry in intertidal sediments: new insights from tidal pools in *Zostera noltei*
941 meadows of Arcachon Bay (France). *Marine Chemistry* 200: 1–13.
942 https://doi.org/10.1016/j.marchem.2018.02.002.
943 Rimmelin, P., J.C. Dumon, E. Maneux, and A. Gonçalves. 1998. Study of annual and seasonal
944 dissolved inorganic nitrogen inputs into the Arcachon Lagoon, Atlantic Coast (France).
945 *Estuarine Coastal Shelf Science* 47(5): 649–659.
946 Saderne, V., P. Fietzek, and P.M.J., Herman. 2013. Extreme Variations of pCO_2 and pH in a
947 Macrophyte Meadow of the Baltic Sea in Summer: Evidence of the Effect of
948 Photosynthesis and Local Upwelling. *PLoS One* 8: e62689.
949 Savelli, R., X. Bertin, F. Orvain, P. Gernez, A. Dale, T. Coulombier, P. Pineau, N. Lachaussée,
950 P. Polsenaere C. Dupuy, and V. le Fouest. 2019. Impact of chronic and massive
951 resuspension mechanisms on the microphytobenthos dynamics in a temperate intertidal
952 mudflat. *Journal of Geophysical Research: Biogeosciences 124*. https://doi.org/10.
953 1029/2019JG005369.
954 Takahashi, T., S.C. Sutherland, C. Sweeney, A. Poisson, N. Metzl, B. Tilbrook, N. Bates, et al.
955 2002. Global sea–air CO_2 flux based on climatological surface ocean pCO_2, and seasonal
956 biological and temperature effects. *Deep Sea Research Part II*: Topical Studies in
957 Oceanography 49: 1601–1622. https://doi.org/10.1016/S0967- 0645(02)00003-6.
958 Ternon Q., P. Polsenaere, V. Le Fouest, J.-B. Favier, O. Philippine, J.-M. Chabirand, J. Grizon,
959 and C. Dupuy. 2018. Étude des pressions partielles et flux de CO_2 au sein de la
960 Communauté d'Agglomération de La Rochelle, rapport scientifique. pp. 32.
961 Vachon, D., Y. T. Prairie, and J. J. Cole. 2010. The relationship between near-surface
962 turbulence and gas transfer velocity in freshwater systems and its effect on floating
963 chamber measurements. *Limnology and Oceanography* 55: 1723–1732.

964 Vaz, L., Frankenbach, S., Serôdio, J., Dias, J.M. 2019. New insights about the primary
965 production dependence on abiotic factors: Ria de Aveiro case study. *Ecological*
966 *Indicators*: 106, 105555, ISSN 1470-160X,
967 https://doi.org/10.1016/j.ecolind.2019.105555.
968 Wang, Z. A. and W.-J. Cai. 2004. Carbon dioxide degassing and inorganic carbon export from
969 a marsh-dominated estuary (the Dublin River): a marsh CO_2 pump. *Limnology and*
970 *Oceanography* 49: 341–354.
971 Wang, Z.A., K.D. Kroeger, N.K. Ganju, M.E. Gonneea, and S.N. Chu. 2016. Intertidal salt
972 marshes as an important source of inorganic carbon to the coastal ocean. *Limnology and*
973 *Oceanography* 61: 1916–1931. https://doi.org/10.1002/lno.10347.
974 Wang, S.R., D. Di Iorio, W.-J. Cai, and C.S. Hopkinson. 2018. Inorganic carbon and oxygen
975 dynamics in a marsh-dominated estuary. *Limnology and Oceanography* 63: 47-71.
976 https://doi.org/10.1002/lno.10614.
977 Wanninkhof, R. 1992. Relationship between gas exchange and wind speed over the ocean.
978 *Journal of Geophysical Research* 97: 7373–7382.
979 Weiss, R.F. 1974. Carbon dioxide in water and seawater: the solubility of a non-ideal gas.
980 *Marine Chemistry* 2: 203–215.
981 Yang C., Telmer K., and Veizer J. 1996. Chemical dynamics of the 'St. Lawrence' riverine
982 system: δH2O, δ^{18}OH2O, δ^{13}CDIC, δ^{34}SSulfate, and Dissolved $^{87}Sr/^{86}Sr$. *Geochimica*
983 *Cosmochimica Acta* 60: 851–866.
984 Yates, K. K., C. Dufore, N. Smiley, C. Jackson, and R. B. Halley. 2007. Diurnal variation of
985 oxygen and carbonate system parameters in Tampa Bay and Florida Bay. *Marine*
986 *Chemistry* 104: 110–124.
987 Zemmelink, H. J., H.A. Slagter, C. van Slooten, J. Snoek, B. Heusinkveld, J. Elbers, N.J. Bink,
988 W. Klaassen, C. J. M. Philippart, and H. J. W. de Baar. 2009. Primary production and

eddy correlation measurements of CO_2 exchange over an intertidal estuary. *Geophysical Research Letters* 36: LI19606. https://doi.org/10.1029/2009GL039285.

Zhang, L., M. Xue, and Q. Liu. 2012. Distribution and seasonal variation in the partial pressure of CO_2 during autumn and winter in Jiaozhou Bay, a region of high urbanization. *Marine Pollution Bulletin* 64: 56–65.

Figure/Table captions

Table 1 Inorganic carbon parameters measured during eight 24 hour-cycles to six 24h and two 12h cycles in the Arcachon flat (44°42.400'N 01°07.500'W) (number of values, mean ± standard deviation in bold and range between brackets). T and S water temperature and salinity, δ^{13}C-DIC dissolved inorganic carbon isotopic ratio, TA total alkalinity, pCO_2 partial pressure of CO_2, and DIC dissolved inorganic carbon. DIC were estimated from measured salinity, temperature, TA and pCO_2 values using the CO_2 system calculation program (Lewis and Wallace 1998) parameterized with the carbonic acid constants sets proposed by Mehrbach et al. (1973) refitted by Dickson and Millero (1987), the borate acidity constant from Lee et al. (2010) and the CO_2 solubility coefficient of Weiss (1974). 15/04/2008 10:00:00 (TU) – 16/04/2008 10:00:00, 02/07/2008 10:00 – 03/07/2008 10:00, 18/09/2008 11:00 – 19/09/2008 11:00, 06/11/2008 08:00 – 06/11/2008 17:00, 29/01/2009 06:00 – 29/01/2009 14:00, 15/04/2009 13:00 – 16/04/2009 13:00, 25/06/2009 06:00 – 26/06/2009 06:00 and 04/09/2009 05:00 – 05/09/2009 05:00. Notice that November 2008 and January 2009 were 12 hour-cycles

Table 2 Gas transfer velocities (k_{600}) and air-sea CO_2 fluxes computed at high tide day and night periods (Fig. 3, the four-hour emerged-periods around low tide at each cycle were removed) for each cycle in the Arcachon flat (mean ± standard deviation and range between

brackets). U_{10} values were computed from wind speed values measured at 9 meters high by the Lège-Cap Ferret Meteo-France station, 12 km far from the 24-H site) using the Amorocho and DeVries (1980) equation. k_{600} values were estimated according to Wanninkhof et al. (1992), Raymond & Cole (2001) and Abril et al. (2009) equations (W92, RC01 and A09, respectively, see M&M). Air-sea CO_2 fluxes were then calculated from k_{600}, water and air pCO_2 values. A mean air pCO_2 value of 390 ppm was chosen according to Eddy Covariance (EC) measurements deployed at 1.8 km far from the tidal creek in 2008 and 2009 (Polsenaere et al. 2012a). For comparison, U_{10} and air-sea CO_2 flux values obtained in July 2008 from simultaneous EC measurements (Polsenaere et al. 2012a) in July 2008 are shown in red. No k_{600} calculations were attempted from these simultaneous EC flux and water pCO_2 measurements at this season due to strong spatial heterogeneity in water bodies highlighted in the present study (see Discussion section 4.4.2.)

Table 3 Seasonal, tidal and diurnal pCO_2 and water-atmosphere variation comparisons across tidal flat, bay, marsh-estuary and mangrove systems of the coastal zone ([a]diurnal and/or tidal, [b]spatial and/or longitudinal sampling methodology)

Table 4 Comparison between day and night pCO_2 values averaged over a same salinity range according to tidal phases (flooding/ebbing) for each 2008-2009 cycle. The non-parametric Mann-Whitney (p-values: *** = 0.0002; **** < 0.0001) test was used. / symbol indicates cycles (flooding and/or ebbing periods) where comparisons were not possible due to not enough data (no data > 5 min. with no significant salinity value difference between day and night periods). To the contrary, time periods (min.) (> 5 min.) where comparisons were possible are specified for each cycle. Temperature comparisons are also given along with the pCO_2 increase or decrease only due to day through nighttime temperature difference (calculated with the CO_2

1039 System Calculation program (version 2.1.) (Lewis and Wallace 1998) from constant T, S, TA
1040 and DIC values measured during each cycle (see Table 1 and M&M section)
1041
1042 **Fig. 1** Localization of the 24 hour-cycle site. (a) The Arcachon lagoon with the subtidal zone
1043 (channels and creeks) and the intertidal mudflat area; (b) the 24 hour-cycle site (24H,
1044 44°42.400'N 01°07.500'W in the subtidal creek always immersed); the EC station (EC,
1045 44°42.9858'N 01°08.6160'W, 1.8 km far from the 24-H site, in the intertidal area emerged for
1046 approximately four hours and immersed for approximately nine hours, Polsenaere et al. 2012a);
1047 the meteo-france station (A) (MF, 44°37.900'N 01°14.900W, 12.450 km far from the 24-H
1048 site). The *Zostera noltei* seagrass meadow is derived from the SPOT image of the 22 June 2005;
1049 it occupies 60 % of the intertidal area (shades of green show the differences in seagrass density,
1050 brown and yellow represent muddy and sandy areas)
1051
1052 **Fig. 2** *In situ* water temperatures (dashed black curve), pCO_2 (black curve with black dots) and
1053 derived temperature-normalized pCO_2 ($NpCO_2$, i.e. pCO_2 variations due to biological activity
1054 or non-temperature effects, black dotted curve with empty black dots, annual mean temperature
1055 over 2008/09 17.7 ± 4.2°C, dotted line) and thermally forced seasonal pCO_2 according to
1056 Takahashi et al. (2002) ($TpCO_2$, i.e. pCO_2 variations due to thermal effects, grey dotted curve
1057 with grey dots, annual mean temperature over 2008/09, 17.7 ± 4.2°C, dotted line and pCO_2 496
1058 ± 36 ppmv, dashed line); mean temperature and pCO_2 over the whole 2008 and 2009 period
1059 were chosen for $NpCO_2$ and $TpCO_2$ computations due to sampled cycle strategy and for better
1060 consistency in year comparisons. Minimum and maximum pCO_2 values (associated to the mean
1061 pCO_2 value) measured during each tidal cycle are also represented (vertical black lines)
1062

1063 **Fig. 3** Tidal and diurnal variations in inorganic carbon and associated parameters measured
1064 during eight 24 hour-cycles to six 24h and two 12h cycles in the Arcachon flat. Water height
1065 (H), salinity (S), temperature (T), partial pressure of CO_2 in the water (pCO_2), total alkalinity
1066 (TA), dissolved inorganic carbon (DIC) and dissolved inorganic carbon isotopic ratio (δ^{13}C-
1067 DIC); (a) 15/04/2008 10:00:00 (TU) – 16/04/2008 10:00:00, (b) 02/07/2008 10:00 – 03/07/2008
1068 10:00, (c) 18/09/2008 11:00 – 19/09/2008 11:00, (d) 06/11/2008 08:00 – 06/11/2008 17:00, (e)
1069 29/01/2009 06:00 – 29/01/2009 14:00, (f) 15/04/2009 13:00 – 16/04/2009 13:00, (g)
1070 25/06/2009 06:00 – 26/06/2009 06:00 and (h) 04/09/2009 05:00 – 05/09/2009 05:00. T and S
1071 were measured every minute by the YSI multiparameter probe on board and H was measured
1072 every hour by the SHOM. The other parameters were sampled on board every hour. Clear and
1073 grey areas represent daytime and nighttime periods, respectively. Notice the same y-axis scale
1074 between cycles was chosen to better see seasonal variations and that November 2008 and
1075 January 2009 were 12 hour-cycles
1076
1077 **Fig. 4** Cross-correlation plots of TA (a), DIC (c) and δ^{13}C-DIC (d) values versus salinity and
1078 apparent 0 end-member versus *in situ* catchment TA value comparison (b). TA versus S slopes
1079 are all significantly positive, DIC versus S slopes are significantly positive except in September
1080 2009 (negative); and δ^{13}C-DIC versus S slopes are positive and significant except in April 2008,
1081 November 2008, September 2009. (b) Apparent 0 end-member TA and *in situ* catchment TA
1082 correspond to Y-intercept of TA versus S cross-correlations and *in situ* TA measurements
1083 carried out at the same time over the Arcachon lagoon watershed watercourses (see Polsenaere
1084 et al. 2012b) computed here as discharge-weighted TA means, respectively
1085
1086 **Fig. 5** Diurnal/tidal plots of water temperature and pCO_2 versus salinity for the four periods:
1087 HT_N high tide at night (dark blue triangle), LT_N low tide at night (green inversed triangle),

LT_D low tide at day (yellow inversed triangle) and HT_D high tide at day (clear blue triangle). (a, b) April 2008, (c, d) July 2008, (e, f) September 2008, (g, h) November 2008, (I, j) January 2009, (k, l) April 2009, (m, n) June 2009 and (o, p) September 2009. Notice the same y-axis pCO_2 scale between all cycles was chosen to better observe diurnal and tidal variations. The same x-axis temperature and salinity scales between April 2008-2009, July 2008-June 2009 and September 2008-2009 were also chosen to better observe variations during the same seasons from 2008 to 2009

Table 1

	T (°C)	*S*	δ^{13}C-DIC (‰)	TA (mmol kg^{-1})	pCO_2 (ppmv)	DIC (mmol kg^{-1})
April 2008	*1441*	*1441*	*23*	*25*	*1441*	*25*
	13.9 ± 0.6	**29.2 ± 0.6**	**-1.1 ± 1.1**	**2.081 ± 0.028**	**474 ± 14**	**1.948 ± 0.024**
	(12.8 ~ 15.4)	(26.2 ~ 30.1)	(-3.7 ~ -0.4)	(2.000 ~ 2.119)	(442 ~ 496)	(1.884 ~ 1.985)
July 2008	*1464*	*1464*	*24*	*25*	*1434*	*25*
	22.2 ± 0.6	**31.2 ± 0.6**	**-0.5 ± 0.4**	**2.131 ± 0.035**	**461 ± 14**	**1.926 ± 0.028**
	(21.2 ~ 23.4)	(30.2 ~ 32.6)	(-1.7 ~ 0.2)	(2.072 ~ 2.211)	(432 ~ 499)	(1.879 ~ 1.995)
September 2008	*1428*	*1428*	*25*	*25*	*1436*	*25*
	19.2 ± 0.2	**33.6 ± 0.3**	**-0.6 ± 0.3**	**2.255 ± 0.021**	**515 ± 36**	**2.062 ± 0.017**
	(18.8 ~ 20.2)	(33.1 ~ 34.5)	(-1.5 ~ -0.1)	(2.223 ~ 2.301)	(405 ~ 597)	(2.017 ~ 2.086)
November 2008	*541*	*541*	*10*	*10*	*541*	*10*
	12.3 ± 0.2	**32.2 ± 0.3**	**-0.6 ± 0.3**	**2.202 ± 0.020**	**463 ± 19**	**2.050 ± 0.022**
	(12.0 ~ 12.6)	(31.8 ~ 32.6)	(-1.3 ~ -0.3)	(2.180 ~ 2.234)	(419 ~ 497)	(2.021 ~ 2.081)
January 2009	*490*	*480*	*9*	*9*	*480*	*9*
	8.9 ± 0.4	**23.2 ± 1.5**	**-1.0 ± 0.5**	**1.646 ± 0.086**	**480 ± 15**	**1.594 ± 0.076**
	(8.3 ~ 10.3)	(20.4 ~ 25.6)	(-2.1 ~ -0.5)	(1.493 ~ 1.733)	(452 ~ 503)	(1.458 ~ 1.669)
April 2009	*1518*	*1518*	*25*	*25*	*1518*	*25*
	13.7 ± 0.3	**30.1 ± 1.0**	**-0.7 ± 0.1**	**2.006 ± 0.053**	**525 ± 14**	**1.891 ± 0.045**
	(12.7 ~ 14.5)	(24.8 ~ 31.5)	(-0.9 ~ -0.5)	(1.840 ~ 2.101)	(494 ~ 568)	(1.752 ~ 1.968)
June 2009	*1441*	*1441*	*24*	*25*	*1441*	*25*

	21.5 ± 0.6	**31.0 ± 0.4**	**-0.2 ± 0.2**	**2.099 ± 0.029**	**490 ± 27**	**1.916 ± 0.023**
	(20.0 ~ 23.3)	(30.2 ~ 32.2)	(-0.4 ~ 0.2)	(2.044 ~ 2.156)	(419 ~ 545)	(1.866 ~ 1.951)
September 2009	*1441*	*1440*	*25*	*25*	*1435*	*25*
	20.9 ± 0.3	**34.0 ± 0.3**	**-0.2 ± 0.3**	**2.218 ± 0.020**	**530 ± 39**	**2.021 ± 0.021**
	(20.2 ~ 21.5)	(33.5 ~ 34.8)	(-0.90 ~ 0.4)	(2.187 ~ 2.251)	(453 ~ 601)	(1.978 ~ 2.051)
2008-2009 Average	*9764*	*9753*	*165*	*169*	*9726*	*169*
	17.7 ± 4.2	**30.5 ± 3.4**	**-0.6 ± 0.4**	**2.079 ± 0.036**	**496 ± 36**	**1.926 ± 0.032**
	(8.3 ~ 23.4)	(20.4 ~ 34.8)	(-3.7 ~ 0.4)	(1.493 ~ 2.301)	(405 ~ 601)	(1.458 ~ 2.086)

Table 2

		U_{10} (m s^{-1})	K_{600} (cm h^{-1})			Air-Sea CO_2 fluxes (mmol m^{-2} h^{-1})		
			W92	RC01	A09	W92	RC01	A09
Apr. 08	*Day*	**4.42 ± 1.42** (2.02 ~ 6.06)	**6.59 ± 3.71** (1.26 ~ 11.37)	**9.9 ± 4.46** (3.87 ~ 15.91)	**17.04 ± 4.92** (8.76 ~ 22.74)	**0.19 ± 0.1** (0.05 ~ 0.34)	**0.29 ± 0.12** (0.14 ~ 0.48)	**0.5 ± 0.12** (0.32 ~ 0.69)
	Night	**2.88 ± 0.7** (2.02 ~ 4.04)	**2.71 ± 1.27** (1.26 ~ 5.05)	**5.38 ± 1.34** (3.87 ~ 7.85)	**11.74 ± 2.4** (8.76 ~ 15.72)	**0.07 ± 0.04** (0.02 ~ 0.14)	**0.13 ± 0.05** (0.07 ~ 0.22)	**0.29 ± 0.11** (0.16 ~ 0.44)
Jul. 08	*Day*	**4.46 ± 2.34** (2.02 ~ 11.1)	**7.71 ± 9.88** (1.26 ~ 38.21)	**14.92 ± 24.73** (3.87 ~ 93.05)	**17.16 ± 8.06** (8.69 ~ 40.09)	**0.18 ± 0.23** (0.03 ~ 0.9)	**0.36 ± 0.58** (0.09 ~ 2.19)	**0.41 ± 0.2** (0.2 ~ 0.94)
	Night	**5.05 ± 1.43** (3.03 ~ 6.06)	**8.37 ± 4.03** (2.84 ~ 11.37)	**12.12 ± 4.94** (5.51 ~ 15.91)	**19.2 ± 4.91** (12.24 ~ 22.68)	**0.21 ± 0.11** (0.07 ~ 0.31)	**0.31 ± 0.13** (0.14 ~ 0.43)	**0.49 ± 0.13** (0.32 ~ 0.61)
EC data Tidal flat	*Day*	**3.86 ± 1.29** (1.29 ~ 7.71)				**-2.25 ± 2.7** (-12.38 ~ 2.1)		
	Night	**4.3 ± 2.21** (0.69 ~ 10.14)				**0.12 ± 1.37** (-2.56 ~ 1.76)		
Sep. 08	*Day*	**2.48 ± 0.83** (1.01 ~ 4.04)	**2.1 ± 1.33** (0.32 ~ 5.05)	**4.72 ± 1.41** (2.72 ~ 7.85)	**10.32 ± 2.86** (5.24 ~ 15.73)	**0.08 ± 0.05** (0.01 ~ 0.16)	**0.19 ± 0.06** (0.1 ~ 0.3)	**0.42 ± 0.15** (0.2 ~ 0.68)
	Night	**2.31 ± 1.39** (1.01 ~ 5.05)	**2.17 ± 2.66** (0.32 ~ 7.9)	**4.82 ± 2.95** (2.72 ~ 11.17)	**9.76 ± 4.81** (5.29 ~ 19.22)	**0.08 ± 0.11** (0.01 ~ 0.32)	**0.19 ± 0.12** (0.09 ~ 0.45)	**0.38 ± 0.19** (0.2 ~ 0.78)
Nov. 08	*Day*	**7.74 ± 1.77** (5.05 ~ 10.09)	**19.37 ± 8.37** (7.9 ~ 31.58)	**33.33 ± 19.51** (11.17 ~ 65.36)	**28.38 ± 6.12** (19.08 ~ 36.54)	**0.53 ± 0.22** (0.25 ~ 0.87)	**0.92 ± 0.52** (0.36 ~ 1.81)	**0.79 ± 0.14** (0.61 ~ 1.01)
	Night							
Jan. 09	*Day*	**2.27 ± 0.97** (1.01 ~ 3.03)	**1.82 ± 1.25** (0.32 ~ 2.84)	**4.4 ± 1.36** (2.72 ~ 5.51)	**9.58 ± 3.3** (5.27 ~ 12.19)	**0.06 ± 0.04** (0.01 ~ 0.11)	**0.14 ± 0.06** (0.08 ~ 0.21)	**0.29 ± 0.13** (0.16 ~ 0.46)
	Night							
Apr. 09	*Day*	**5.35 ± 3.37** (1.01 ~ 10.09)	**12.03 ± 12.55** (0.32 ~ 31.58)	**22.84 ± 25.61** (2.72 ~ 65.36)	**20.02 ± 11.43** (5.24 ~ 36.09)	**0.56 ± 0.59** (0.01 ~ 1.59)	**1.06 ± 1.2** (0.12 ~ 3.3)	**0.93 ± 0.55** (0.23 ~ 1.82)
	Night	**4.04 ± 1.81** (2.02 ~ 7.07)	**5.9 ± 5.23** (1.26 ~ 15.48)	**9.43 ± 6.95** (3.87 ~ 22.65)	**15.58 ± 6.18** (8.65 ~ 25.9)	**0.23 ± 0.2** (0.06 ~ 0.6)	**0.38 ± 0.26** (0.18 ~ 0.87)	**0.63 ± 0.21** (0.4 ~ 1)
Jun. 09	*Day*	**3.62 ± 1.32** (1.01 ~ 5.05)	**4.55 ± 2.65** (0.32 ~ 7.9)	**7.39 ± 2.92** (2.72 ~ 11.17)	**14.18 ± 4.51** (5.25 ~ 19.06)	**0.13 ± 0.08** (0.01 ~ 0.25)	**0.22 ± 0.09** (0.09 ~ 0.35)	**0.43 ± 0.14** (0.17 ~ 0.6)
	Night	**3.7 ± 1.17** (3.03 ~ 5.05)	**4.53 ± 2.92** (2.84 ~ 7.9)	**7.4 ± 3.27** (5.51 ~ 11.17)	**14.54 ± 4.02** (12.21 ~ 19.18)	**0.12 ± 0.08** (0.07 ~ 0.22)	**0.2 ± 0.09** (0.13 ~ 0.31)	**0.4 ± 0.12** (0.29 ~ 0.53)
Sep. 09	*Day*	**9.31 ± 3.1** (5.05 ~ 13.12)	**29.51 ± 18.64** (7.9 ~ 53.37)	**81.73 ± 80.78** (11.17 ~ 188.61)	**32.09 ± 10.07** (19.18 ~ 46.85)	**1.02 ± 0.65** (0.23 ~ 1.83)	**2.8 ± 2.68** (0.32 ~ 6.48)	**1.11 ± 0.47** (0.48 ~ 1.65)
	Night	**2.88 ± 0.91** (2.02 ~ 4.04)	**2.8 ± 1.7** (1.26 ~ 5.05)	**5.48 ± 1.78** (3.87 ~ 7.85)	**11.71 ± 3.14** (8.71 ~ 15.75)	**0.11 ± 0.06** (0.05 ~ 0.21)	**0.23 ± 0.06** (0.14 ~ 0.33)	**0.49 ± 0.11** (0.32 ~ 0.66)

1126

1127

1128

1129

1130 **Table 3**

1131

Study Site	Seasonal pCO_2 range (ppmv)	Diurnal-tidal pCO_2 range (ppmv)	Water-atmosphere CO_2 flux (mmol m^{-2} h^{-1})	Reference
Arcachon tidal flat (France)	461 ± 14 (July 2008) – 530 ± 39 (September 2009)	(452 - 503) (January 2009) to (405 - 597) (September 2008)	0.27 ± 0.22 to 0.56 ± 0.54	This study[a]
Aiguillon tidal flat (France)	(390 - 609) (spring - summer 2017) (215 - 1929) (summer - fall 2018)		0.14 (-0.075 to 1.13, summer - winter)	Polsenaere et al. (2018)[b]; Coignot et al. (2020; in prep.)[b]
Aiguillon tidal flat (France)		(466 - 1024) (HT-LT) (summer 2018)	1.00 ± 0.82	Ternon et al. (2018)[a]
Duplin River salt marsh-estuary (Georgia, USA)		(500 - 4000) (HT-LT, winter) to (1600 - 12,000) (HT-LT, summer) (2014)	-0.7 to -5.5 and -0.6 to -3.9	Wang et al. (2018)[a,b]
Tidal marsh channel of the Fier d'Ars (Ré Island, France)	385 ± 60 (267 - 522) (summer) to 460 ± 58 (334 - 569) (autumn)	(377 - 510) (HT-LT, winter 2018) to (334 - 569) (HT - LT, Autumn 2018)	-0.18 ± 0.18 (spring) to 0.10 ± 0.08 (winter)	Mayen et al. (in prep.)[a]
Amazon estuary - tidal forest channel		5000 ± 300 - 2320 ± 40 (LT - HT, February 2007)		Abril et al. (2013)[a]
Ras Dege (Tanzania) mangrove creek		500 - 5000 (September 2005)	0.04-3.33	Bouillon et al. (2007)[a]
Nagada (Papua New Guinea) and the Gaderu (India) mangrove creeks		(540 - 1680) and (1380 - 4770) (July, August 2000)	1.82 ± 1.38 and 2.33 ± 4.20	Borges et al. (2003)[a]
Bay of Brest (subtidal)	200 - 700 (summer-winter, 2013 to 2010)		-0.0083 to -0.38 (spring and summer) and 0.038 to 0.91 (fall and winter)	Bozec et al. (2011)[a]
Estuary of Guadalquivir Estuary and the Bay of Cadiz	341 ± 18 (February 2007) - 411 ± 20 (November 2006)		-0.058 (February 2007) and 0.15 (November 2006)	Ribas-Ribas et al. (2011)[b]
Coastal systems of Cadiz Bay (Spain)		(589 - 1244), (525 - 1405) and (742 - 1059) (HT-LT, summer 2015)	0.375 to 2.37	Burgos et al. (2018)[a,b]
Jiaozhou Bay (East China Sea)	315 - 720 (autumn 2007) and 145 - 315 (winter 2008)		0.12 (autumn) and -0.68 (winter)	Zhang et al. (2012)[b]
Tampa and Florida bays (US)	414 ± 86 (October 2003); 351 ± 72 (March 2000)	(262 - 580) (October 2003); (260 - 497) (March 2000)		Yates et al. (2007)[a]
Macrophyte meadow (Baltic Sea)		281 ± 88 (July); 219 ± 24 (August); 1488 ± 574 (September 2011)		Saderne et al. (2013)[a]
Zostera marina meadow, Eastern shore of Virginia (US)	425 (April) - 490 (June 2015)	(193 - 731) (April); (256 - 859) (June 2015)		Berg et al. (2019)[a]
Guanabara Bay (Brazil)	353 ± 141 and 194 ± 127 (S3); 380 ± 286 and 203 ± 159 (S4); 364 ± 343 and 132 ±	591 ± 231 to 194 ± 114 (September 2013); 163 ± 40 to 116 ± 25 (January 2014); 346 ± 166 to 146	-2.87 (S3); -2.16 (S4); -2.52 (S5)	Cotovicz et al. (2015)[a,b]

	74 (S5) (winter and summer)	± 106 (February 2014); 637 ± 421 to 265 ± 186 (April 2014) (S4, S5)

Table 4

		Day			Night			Significant differences (Day vs Night)			pCO_2 increase or decrease only due to day through night T difference
		Salinity	pCO_2 (ppmv)	T (°C)	Salinity	pCO_2 (ppmv)	T (°C)	Salinity	pCO_2	T	
Apr. 2008	**Flooding**	/	/		/	/		/	/	/	/
	Ebbing (30 min.)	29.27	481	14.47	29.27	471	13.56	No	Yes ****	Yes ****	-18
Jul. 2008	**Flooding**	/	/		/	/		/	/	/	/
	Ebbing (10 min.)	30.4	493	21.35	30.43	471	22.55	No	Yes ****	Yes ****	+21
Sept. 2008	**Flooding (120 min.)**	33.55	513	18.95	33.55	537	19.07	No	Yes ****	Yes ****	+2
	Ebbing	/	/		/	/		/	/	/	/
Nov. 2008	**Flooding**	/	/		/	/		/	/	/	/
	Ebbing	/	/		/	/		/	/	/	/
Jan. 2009	**Flooding**	/	/		/	/		/	/	/	/
	Ebbing	/	/		/	/		/	/	/	/
Apr. 2009	**Flooding**	/	/		/	/		/	/	/	/
	Ebbing	/	/		/	/		/	/	/	/
Jun. 2009	**Ebbing**	/	/		/	/		/	/	/	/
	Flooding	/	/		/	/		/	/	/	/
Sept. 2009	**Flooding (30 min.)**	33.89	552	20.97	33.9	572	20.58	No	Yes ***	Yes ****	-8
	Ebbing (15 min.)	33.97	540	20.97	33.96	535	20.84	No	Yes ***	Yes ****	-3

Fig. 1

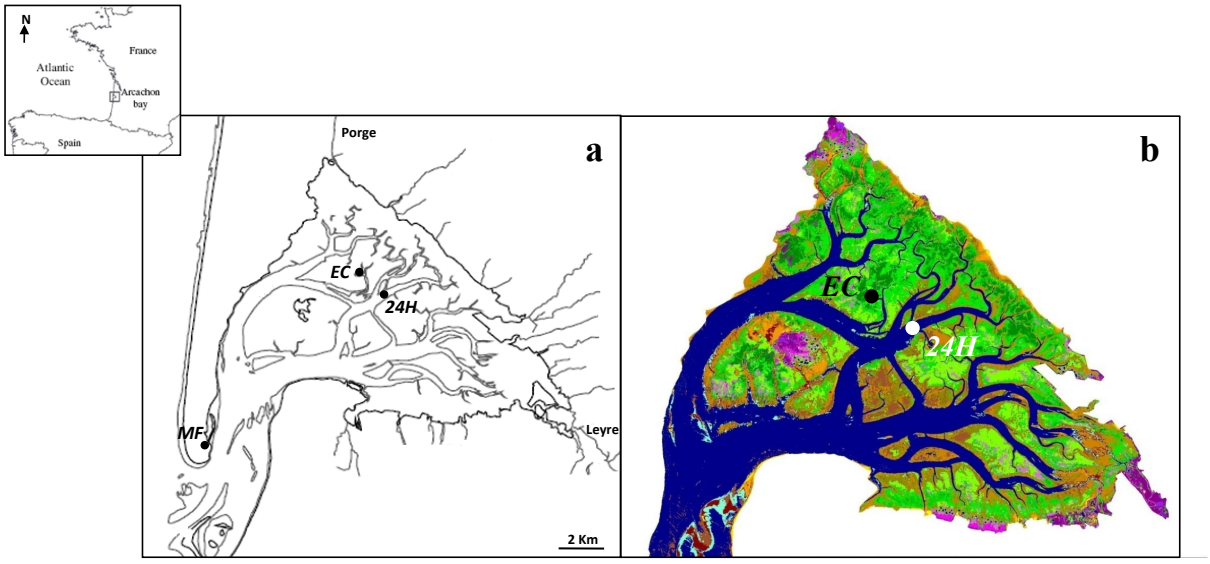
N
France
Atlantic Ocean
Arcachon bay
Spain
Porge
a
EC
24H
MF
Leyre
2 Km
b
EC
24H

Fig. 2

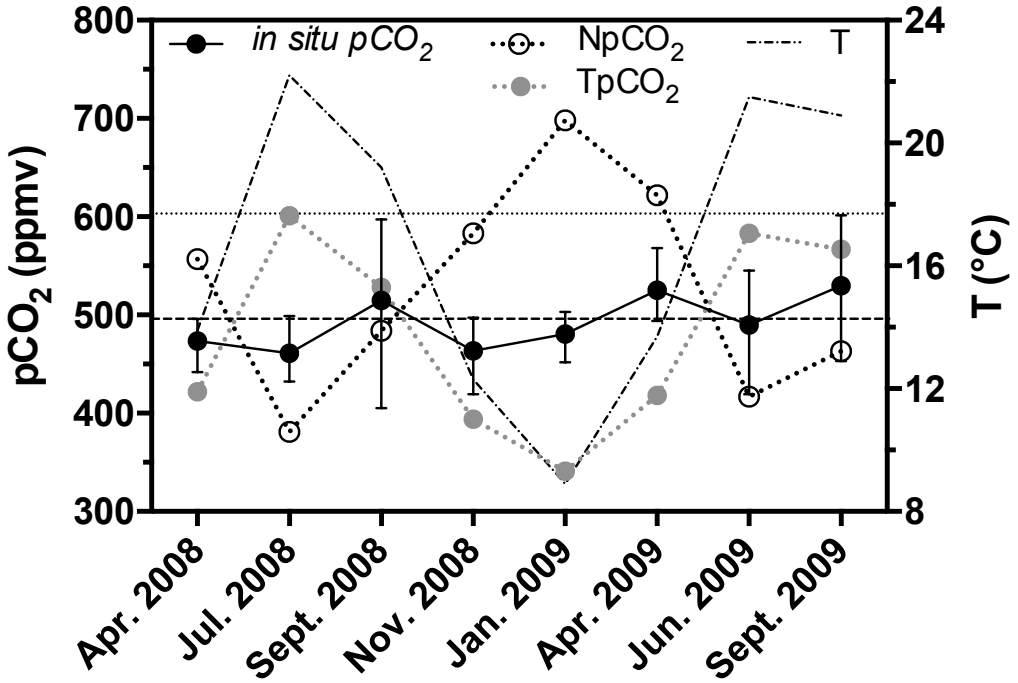
800
700
600
500
400
300
24
20
16
12
8
in situ pCO2
NpCO2
TpCO2
T
pCO2 (ppmv)
T (°C)
Apr. 2008
Jul. 2008
Sept. 2008
Nov. 2008
Jan. 2009
Apr. 2009
Jun. 2009
Sept. 2009

Fig. 3

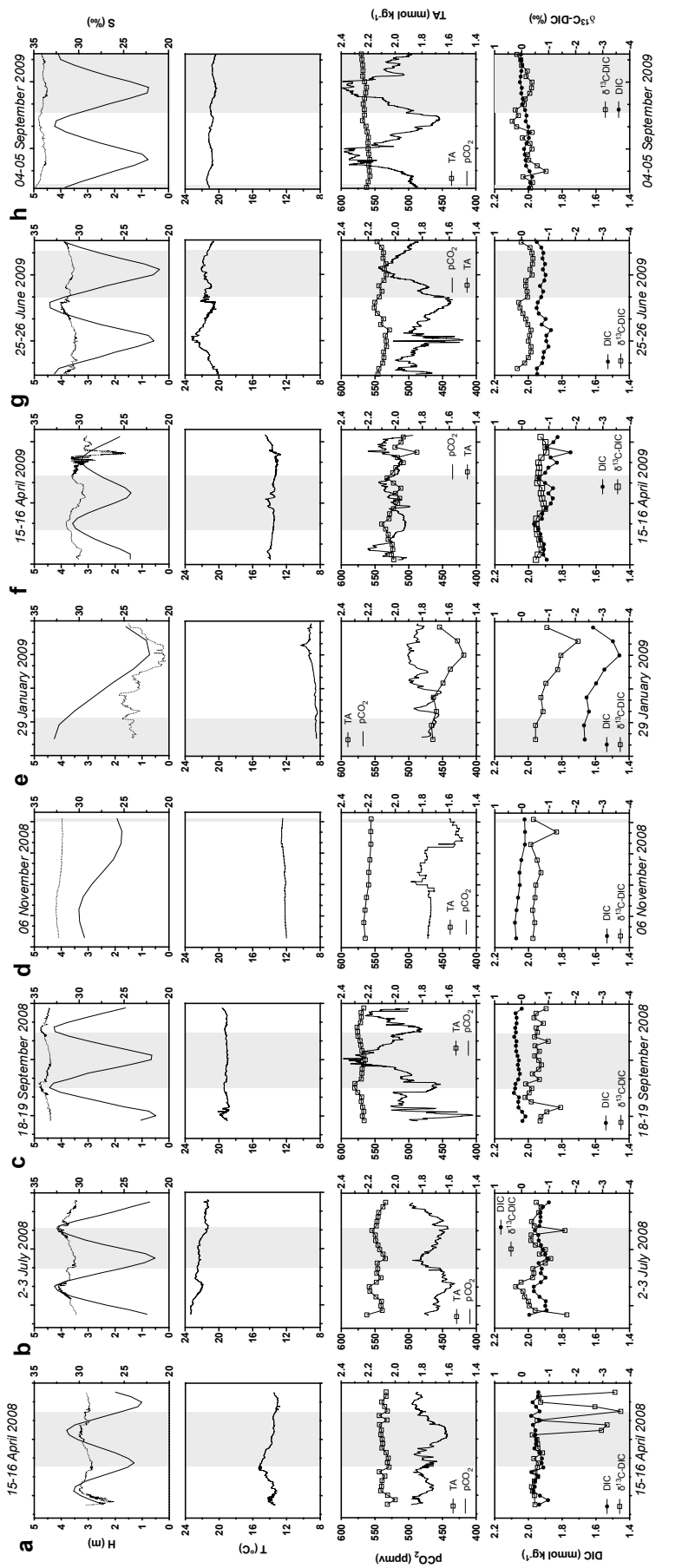
a
b
c
d
e
f
g
h
15-16 April 2008
2-3 July 2008
18-19 September 2008
06 November 2008
29 January 2009
15-16 April 2009
25-26 June 2009
04-05 September 2009
H (m)
T (°C)
pCO2 (ppmv)
TA (mmol kg-1)
S (‰)
DIC (mmol kg-1)
δ13C-DIC (‰)
TA
pCO2
DIC
δ13C-DIC

Fig. 4

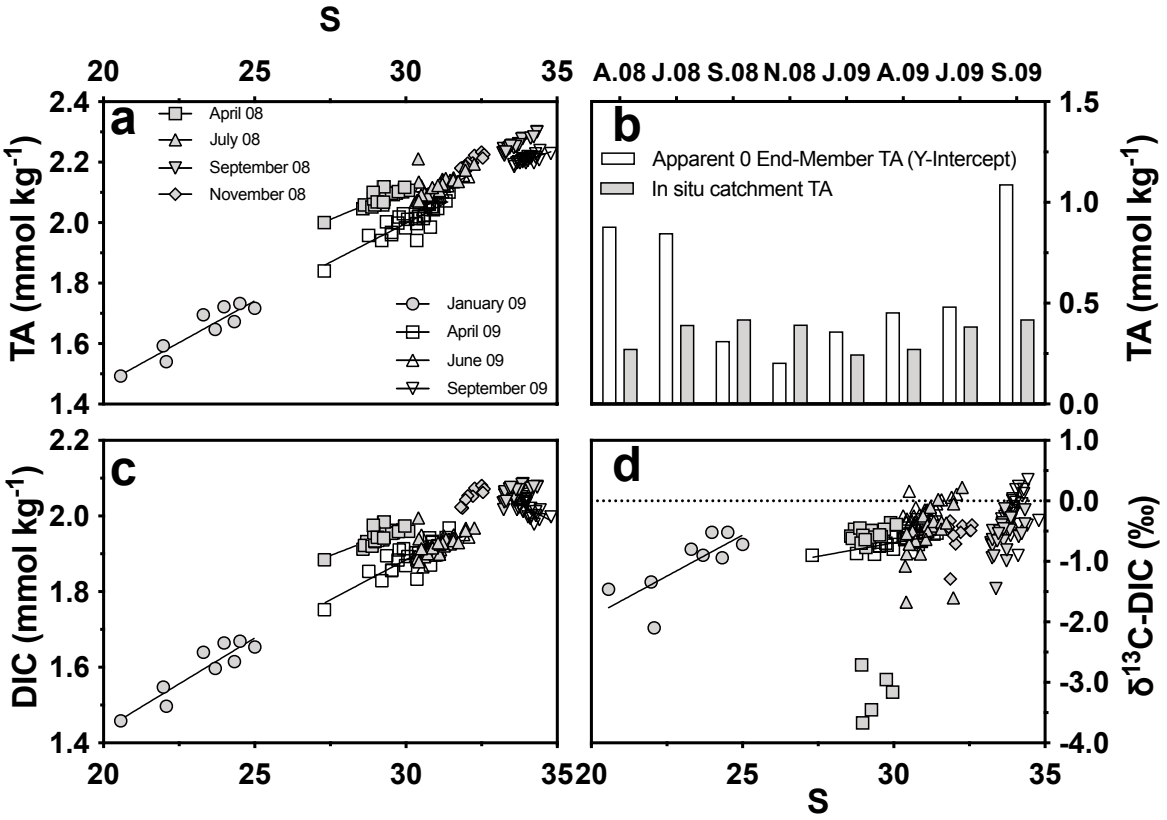
S
20
25
30
35
A.08 J.08 S.08 N.08 J.09 A.09 J.09 S.09
a
April 08
July 08
September 08
November 08
January 09
April 09
June 09
September 09
TA (mmol kg-1)
b
Apparent 0 End-Member TA (Y-Intercept)
In situ catchment TA
c
DIC (mmol kg-1)
d
δ13C-DIC (‰)

Fig. 5

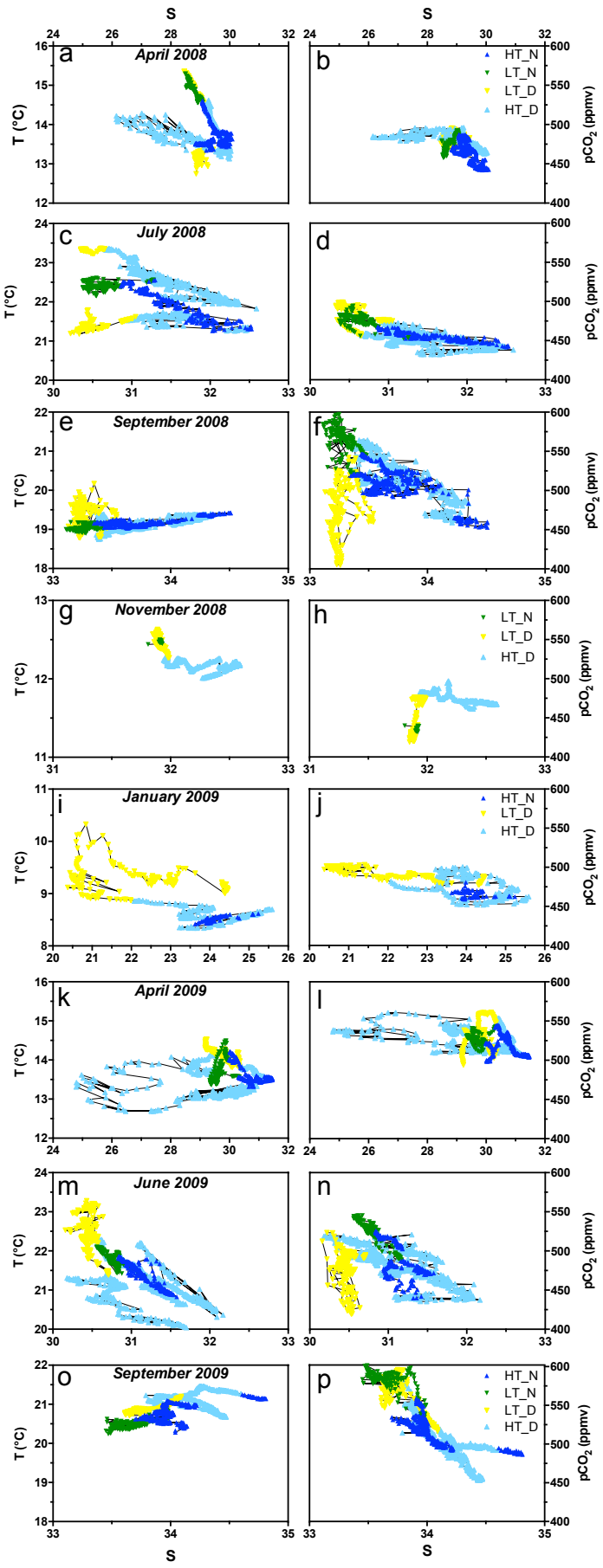
a
April 2008
b
HT_N
LT_N
LT_D
HT_D
c
July 2008
d
e
September 2008
f
g
November 2008
h
i
January 2009
j
k
April 2009
l
m
June 2009
n
o
September 2009
p
T (°C)
pCO2 (ppmv)
S

1238

1239